2.75

Geochemical Halos in the Silver City Mining Region and Adjacent Areas, Grant County, New Mexico

GEOLOGICAL SURVEY BULLETIN 1534

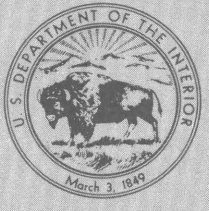

ERRATA

U.S. GEOLOGICAL SURVEY BULLETIN 1534

Geochemical Halos in the Silver City Mining Region and Adjacent Areas, Grant County, New Mexico

The map on p. 56, now labeled figure 15, actually shows the distribution of gold (nonmagnetic fraction) not silver (magnetic fraction). The map on p. 58, now labeled figure 16, actually shows the distribution of silver (magnetic fraction) not gold (nonmagnetic fraction). The figure captions, text references to the figures, and the table of contents are correct; only the corresponding maps have been reversed.

Geochemical Halos in the Silver City Mining Region and Adjacent Areas, Grant County, New Mexico

By KENNETH C. WATTS, JERRY R. HASSEMER, *and* DAVID F. SIEMS

GEOLOGICAL SURVEY BULLETIN 1534

UNITED STATES GOVERNMENT PRINTING OFFICE, WASHINGTON: 1984

UNITED STATES DEPARTMENT OF THE INTERIOR

WILLIAM P. CLARK, *Secretary*

GEOLOGICAL SURVEY

Dallas L. Peck, *Director*

Library of Congress cataloging in Publication Data

Watts, K. C.
Geochemical halos in the Silver City mining region and adjacent areas, Grant County, New Mexico.
(Geological Survey Bulletin 1534)
Bibliography: 85 p.
Supt. of Docs. no.: I 19.3:1534
1. Geochemistry—New Mexico—Grant County. 2. Ore deposits—New Mexico—Grant County.
I. Hassemer, Jerry R. II. Siems, David F. III. Title. IV. Series.

QE75.B9 no. 1534 557.3s [553.4'09789'692] 81-607560
[QE515] ACR2

For sale by the Branch of Distribution, U.S. Geological Survey
604 South Pickett Street, Alexandria, VA 22304

CONTENTS

ILLUSTRATIONS

[Figures 3–22 follow text]

TABLES

[Tables follow text]

GEOCHEMICAL HALOS IN THE SILVER CITY MINING REGION AND ADJACENT AREAS, GRANT COUNTY, NEW MEXICO

By KENNETH C. WATTS, JERRY R. HASSEMER, and DAVID F. SIEMS

ABSTRACT

An alluvial heavy-mineral survey of the Silver City mining region and adjacent areas, Grant County, N. Mex., was completed in 1976. Geochemical data resulting from this survey show areas of anomalous metals that conform to geologic control. Anomaly patterns indicate that some of these areas may contain additional economic mineral deposits; other areas probably constitute zones of subeconomic, dispersed concentrations of metals that nevertheless record the regional pathways along which mineralizing solutions were channeled and ore metals and gangue mineral products of hostrock alteration were deposited.

The geochemical maps suggest some new exploration targets, one of the most promising of which is the area surrounding Fleming Camp, an old silver district of modest production history. Geochemical evidence at Fleming Camp suggests the presence of a buried intrusive cupola that has caused skarn development and perhaps controlled associated metallization of which the silver deposits are a part. This inference is based on comparison of the geochemical anomalies at Fleming Camp with those in the Pinos Altos district where large tonnages of skarn-associated replacement deposits are known. Similarities in metals present, in anomaly strength, and in areal extent indicate that deposits of similar genetic origin to those at Pinos Altos may exist at depth near Fleming Camp.

The geochemical characteristics of 11 areas were compared using U.S. Geological Survey STATPAC computer programs. The relative effects of weathering, and amounts of pyrite as reflected by amounts of supergene dispersion, and the extent to which the chalcophilic elements are fixed by secondary iron-manganese oxides were compared between areas by using a ratio of fraction magnitude of the iron and manganese oxide rich, heavy-mineral magnetic component to that of the iron and manganese oxide poor nonmagnetic component, which is usually more rich in primary and secondary ore minerals. The ratio provides an index that allows the areas to be compared and ranked relative to the importance of supergene processes.

Possible levels of erosion relative to inner metal zones were assessed in several areas by using an element magnitude (EM) measurement (element intensity × size halo area), which provided an index of the importance of the supraore (usually peripheral metals in a zonation sequence) in each area in relation to the importance of subore (usually inner metal zone) metals based on the additive ratio of the EM values: (Pb + Ag + Ba)/(Cu + Mo + Bi), in the mechanically dispersed ore mineral (nonmagnetic) fraction. The ranking derived from using these ratios placed the erosion levels of the Georgetown and Fleming Camp districts above those of the inner, possibly main ore zones, on the basis of the large supraore component, and placed the erosion levels at the Fierro-Hanover district near the roots of the inner ore zone of its metal system, as suggested by a dominant subore component (low ratio). All other windows were in sequence between these extremes.

INTRODUCTION

The numerous geochemical anomalies detected in the Silver City mining region and adjacent areas, Grant County, N. Mex., are discussed in this report, and the possible significance of the anomalies is evaluated. The anomalies (also called "halos"; see description following) were noted in 1976 during a geochemical study in eight contiguous 7½-minute quadrangles near Silver City. A statistical summary and listing of the analytical data from this sampling program are contained in Open-File Report 78-801 by Watts, Hassemer, Siems, and Nishi (1978b).

A halo is defined in this report as an anomalous geochemical pattern of variable symmetry that relates to either an economic mineral deposit or to epigenetically dispersed metals in subeconomic but anomalous concentrations. Many of the halos discussed in this report are asymmetrical or linear in shape because they often reflect metals localized by linear, structural weaknesses in the rocks, such as faults, dikes, and fractures. Sometimes the linearity and asymmetry are not attributable to observable features on the surface, indicating the presence of causative geologic features in the subsurface. Common practice reserves the use of the word halo to those geochemical anomalies associated with economic mineral deposits and has implied that halos of this type are at least nearly symmetrically disposed about the deposits. A metal dispersion halo according to common usage can be of several types: It may be called "primary," if it formed at the time of hypogene metallization; "leakage," if it developed in overlying rocks during or shortly after a mineral deposit is formed; or "secondary," if it resulted from the supergene destruction of a mineral deposit (Beus and Gregorian, 1977; Hawkes and Webb, 1962; Levinson, 1974). All these types occur in the Silver City area, and many of them probably conform and overlap with each other; but because additional factors contribute to the formation of an economic mineral deposit, beyond the introduction of metals by mineralizing solutions, all halos need not be related to deposits of ore grade. The halos described in this report show only that many metals were epigenetically introduced over broad areas and were made available for economic accumulation, whether or not favorable environments were present.

The area of study, which is between lat 32°45'00" N. and 33°00'00" N. and long 108°00'00" W. and 108°30'00" W. in Grant County, N. Mex. (fig. 1), is in general subdivisible into two geologic and physiographic areas. Portions north of about lat 32°52'30" N., which are relatively high in elevation, are underlain by middle Tertiary volcanic rocks. Areas south of this latitude are referred to as the

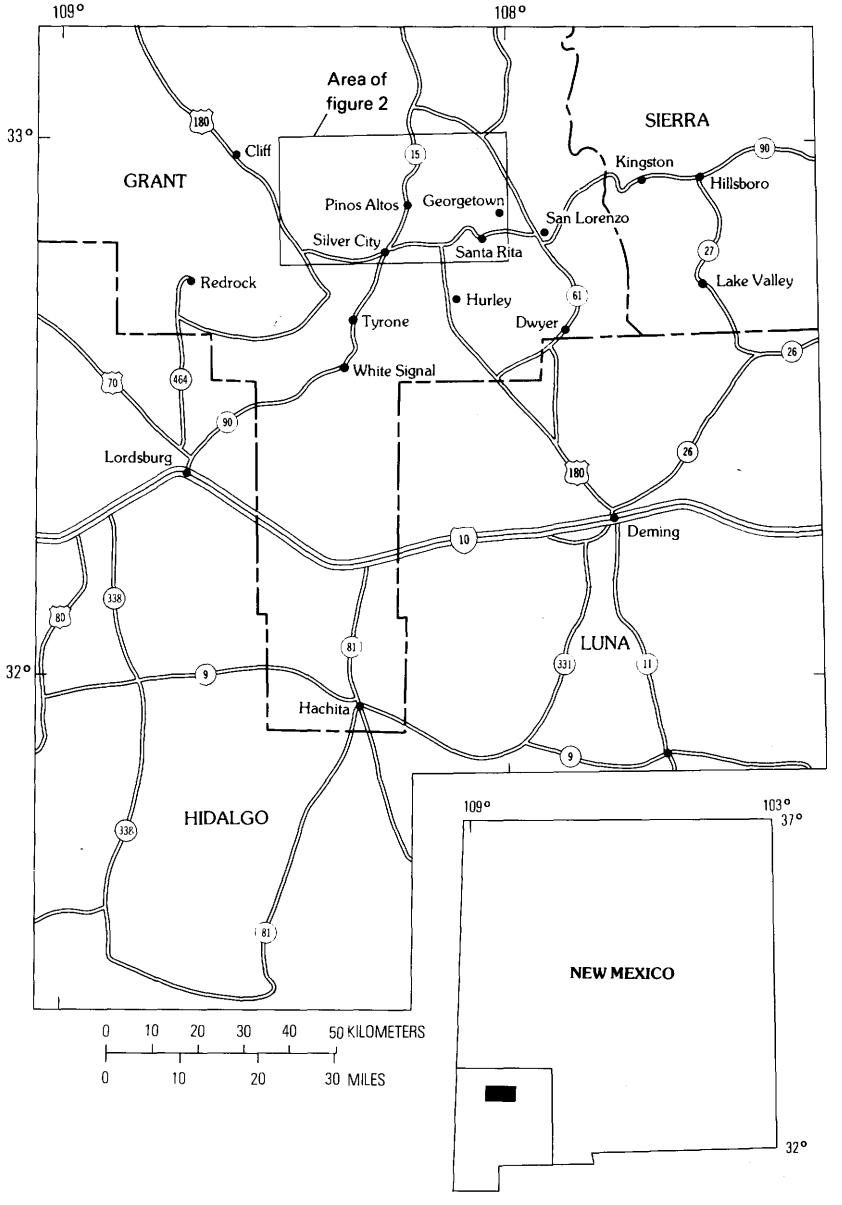

FIGURE 1.—Index map showing location of study area.

Silver City mining region; here, erosion has removed the middle Tertiary volcanic cover and has exposed rocks ranging in age from Precambrian to early Tertiary. The Silver City mining region, which is highly mineralized, contains several exposed, economically signifi-

cant metal-producing districts. They include (1) the disseminated and replacement copper deposits at Santa Rita, (2) the iron-zinc skarn-replacement deposits at and between Fierro and Hanover, (3) the vein and vein-replacement zinc-lead-copper-silver deposits at Central, (4) the vein-replacement silver deposits at Georgetown, (5) the gold-silver vein and skarn-replacement zinc-copper-lead deposits of Pinos Altos, (6) the vein-replacement silver deposits at Chloride Flat, (7) the vein-replacement manganese-iron deposits at Boston Hill, and (8) the vein-replacement silver deposits at Fleming Camp.

In the terrain north of the Silver City mining region, the middle Tertiary volcanic cover obscures whatever Laramide mineral deposits may exist in the older rocks below, though younger, mid-Tertiary deposits may occur within or below the volcanic pile. It is also possible that the imprints of waning stages of Laramide metallization may be present.The volcanic terrane afforded an opportunity to test methods of exploring with geochemistry for covered mineral deposits beneath and within a volcanic pile adjacent to a major mineralized region of similar history but with a deeper exposure. There may have been some success.

A particularly striking characteristic of the geochemical anomaly patterns both within the mining region and the volcanic terrane is their continuity, in the case of some metals, transecting all lithologic boundaries, and the erosional boundary between the two contrasting terranes. Geochemical patterns in the Silver City mining region suggest that epigenetic metallization took place in a vast, interrelated network controlled by zones of faults and perhaps closely spaced fractures, the dominant trends of which are north, northeast, and northwest. The fact that linear anomaly patterns are more numerous than known faults, but similarly oriented, indicates that they may provide a more complete representation of the hydrothermal conduit system than does the mapped geology. Dispersed metallization is defined by Beus and Grigorian (1978, p. 281) as noneconomic concentrations of elements and minerals that are formed as a result of ore-fluid effects on enclosing rocks. Many of the geochemical patterns in the study area probably reflect dispersed metallization, but they nevertheless appear to record solution pathways, which in itself can be a useful exploration tool. Where these dispersed metallizations encounter favorable environments, however, economic concentrations can develop. Empirical observations indicate that some of the most favorable environments are found where the geochemical anomaly patterns intersect, which in many cases also corresponds with areas of known deposits. The intersections of geochemical patterns probably record zones within the network of conduits where regional dilational forces allowed more efficient mineral deposition.

The variety of plutonic rocks, many with associated ore deposits, and a rather well-defined structural pattern that seems to have controlled ore deposition make the study region ideally suited for comparing selected areas on the basis of geochemical characteristics; the purpose being that comparisons can be used to investigate methods of assigning sequential exploration priorities to geochemical anomalies, using as criteria types of deposits potentially present and erosion levels that probably exist relative to inner or main ore zones.

ACKNOWLEDGMENTS

Several members of the U.S. Geological Survey contributed to this study in both the field and the laboratory. In particular, the efforts of James Nishi, who performed some of the spectrographic analyses, Richard Babcock, and Dwight Rhiner, who assisted in laboratory and field, are greatly appreciated. We also gratefully acknowledge the friendly cooperation extended by numerous landowners in the area. Special acknowledgment is made to D. H. Richter and G. B. Gott whose very helpful comments and constructive criticism improved this report considerably during the review process.

GEOLOGIC SETTING

The older rocks exposed south of lat 32°52′30″ N. consist of Proterozoic Y granite, Paleozoic carbonate rocks and shale, and Mesozoic shale, mudstone, and volcanic rocks (fig. 2). These rocks are exposed on a broad northwest-trending syncline that is cut by numerous, chiefly normal faults, and is intruded by a complex sequence of mafic-felsic dikes, sills, and stocks of Cretaceous to middle Tertiary age. The stocks are important loci for mineral deposits and include such bodies as: (1) the Santa Rita granodiorite porphyry stock, (2) the Fierro-Hanover granodiorite-quartz diorite pluton, (3) the Pinos Altos quartz monzonite stock, and (4) the Silver City granodiorite stock (Trauger, 1972; Cunningham, 1974; Jones and others, 1967; Hernon and others, 1953; Jones and others, 1970).

The Tertiary volcanic rocks north of about lat 32°52′30″ N. are composed mostly of ash-flow tuff units of Oligocene age (Finnell, 1976a, b; Trauger, 1972; Moore, 1953), which are intruded by dikes and by shallow, irregular bodies of felsic composition. Normal faulting cuts the volcanic units into a series of northwest-trending horsts and grabens.

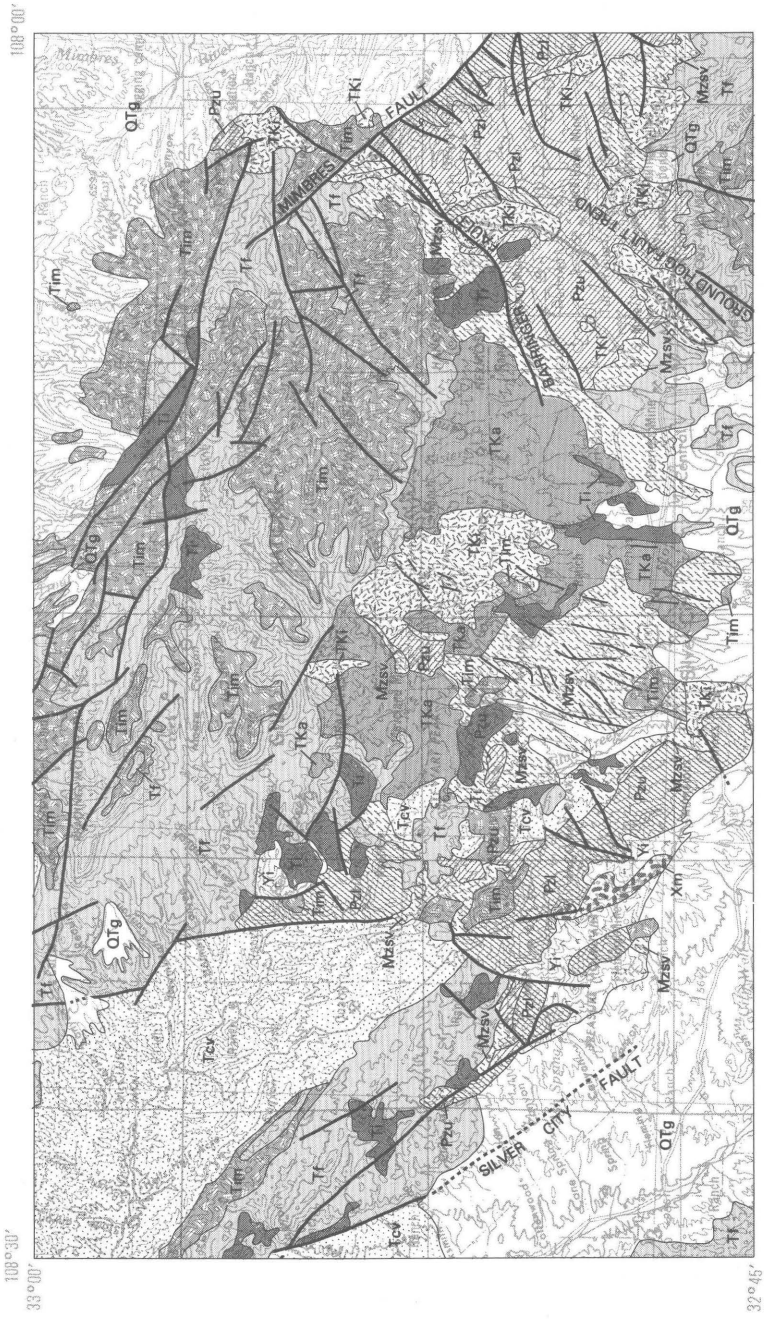
108°00'
108°30'
33°00'
32°45'
Mimbres
River
QTg
Tim
Tf
TKi
TKa
Pzu
Mzsv
Tcv
Yf
Xm
MIMBRES FAULT
SILVER CITY FAULT
GROUNDHOG FAULT
BAYARD

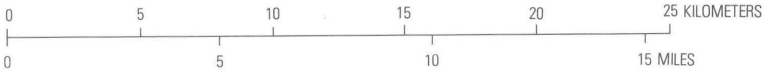

EXPLANATION

QTg — GRAVEL, SAND, SILT, AND CLAY (QUATERNARY AND TERTIARY)—Mainly alluvium on stream terraces, fan aprons, and pediments; colluvium on hill slopes; and lacustrine and eolian deposits in basins

Tcv — CONGLOMERATE AND VOLCANIC ROCKS (TERTIARY)—Mainly coarse conglomerate with intercalated mafic to intermediate flows and tuff

Tim — INTERMEDIATE TO MAFIC VOLCANIC ROCKS (TERTIARY)—Mainly flows, scoria cones, domes, and small intrusions. Locally includes small units of felsic volcanic rocks and volcaniclastic rocks

Tf — FELSIC VOLCANIC ROCKS (TERTIARY)—Mainly flows, domes, and pyroclastic deposits. Locally includes small units of mafic volcanic rocks and volcaniclastic rocks

Ti — INTRUSIVE ROCKS (TERTIARY)—Includes granitic rocks in plutons and aphanitic and porphyritic rocks in plugs and dikes

TKi — INTRUSIVE ROCKS (TERTIARY AND CRETACEOUS)—Includes granitic rocks (commonly porphyritic) in plutons and porphyritic rocks and breccias in dikes, plugs, and small stocks

TKa — ANDESITIC ROCKS (TERTIARY AND CRETACEOUS)—Flows and small intrusions. Locally includes beds of sedimentary rocks

Mzsv — SEDIMENTARY AND VOLCANIC ROCKS (MESOZOIC)—Mainly shale, siltstone, sandstone, and conglomerate; includes some limestone and felsic to intermediate volcanic rocks. Mainly Bisbee Group to the southwest and Colorado Formation to the northeast, both of Cretaceous age

Pzu — SEDIMENTARY ROCKS, UPPER PART (PERMIAN AND PENNSYLVANIAN)—Mainly limestone; includes some dolomite and sandstone. Chiefly Naco Group

Pzl — SEDIMENTARY ROCKS, LOWER PART (MISSISSIPPIAN AND CAMBRIAN)—Mainly limestone, dolomite, shale, quartzite, and sandstone; includes some conglomerate and arkose

Yr — INTRUSIVE ROCKS (PROTEROZOIC Y)—Granitic rocks, commonly porphyritic or porphyroblastic, in plutons

Xp — METASEDIMENTARY AND METAIGNEOUS ROCKS (PROTEROZOIC X)—Includes Pinal Schist, gneisses

CONTACT

NORMAL FAULT—Dotted where concealed

DIKE (TERTIARY AND CRETACEOUS)—Mafic porphyry, dominantly quartz diorite

FIGURE 2.—Generalized geologic map of the Silver City mining region and adjacent areas, Grant County, N. M. Modified from map compiled by Silver City 1° × 2° quadrangle, conterminous United States Mineral Appraisal Program team, unpublished mapping 1980.

GEOCHEMICAL INVESTIGATIONS

SAMPLE MEDIUM AND METHODS

This study used panned heavy minerals derived from active alluvium as the basic sample medium. The alluvium was derived nearly exclusively from unbranched stream tributaries within areas of bedrock outcrop. This sampling approach has been somewhat effective in other parts of the southwestern United States for both regional and relatively detailed district studies. Two factors are responsible for the effectiveness of the geochemical sample medium: First, the metals released during destruction of the mineral deposits are more commonly dispersed mechanically than chemically in the semiarid environment; and second, most mechanically dispersed, ore-related metals occur in minerals and limonitic aggregates of specific gravity greater than 2.8, which makes them amenable to collection into a heavy-mineral concentrate.

The samples were collected from 921 localities, from ephemeral streams that were short in length and small in drainage area (often <3 km^2). Small drainage basins were selected because mechanical-dispersion trains rarely exceed 2.5 km in arid or semiarid regions (Beus and Grigorian, 1977, p. 198), because contamination from mining and milling, which is cumulative in drainage systems, is more likely to be a problem in large drainage basins, and because the details of the metal dispersion can be gained by the relatively detailed sampling small drainages offer.

Each sample was collected at oblique angles to the active drainage channel and as near to underlying bedrock as possible. Composite samples were collected randomly across the full width of wide active channels where such channels were present. Occasionally, extensive boulder and cobble rubble required compositing of sediment from various accumulations behind rocks and in potholes. These bulk samples, which weighed from 4 to 5 kg, were then gold panned on site if water was available, or otherwise they were carried away from the site to be panned later. Panning was done to the point where the sample reduced to heavy minerals and to a light-mineral diluent content of about 30 percent; the size of the heavy-mineral sample after removal of diluent—when uniform amounts of sediment are initially collected—is determined mostly by the geology of the basin area and therefore is highly variable. Samples from Fort Bayard quadrangle were consistently larger than average because of the abundant, clastic ferromagnesium minerals derived from the numerous mafic dikes in the area.

Further processing of the sample after panning consisted of drying, magnetite removal, bromoform separation to remove the light-mineral diluent, magnetic separation at 1.0 A (25 degree forward, 15 degree side-slope, using a Frantz Isodynamic Separator[1]) into two fractions, and then pulverization to a fine powder. These methods have been described in more detail by Watts, Hassemer, Siems, and Nishi (1978b).

Magnetic separation of the heavy minerals provides interpretational advantages. The magnetic field intensities and slope settings nearly separate the sample into components of light- and dark-colored minerals. The nonmagnetic (at 1.0 A) component contains light-colored rock-accessory minerals and most ore-related primary and secondary minerals; whereas, the magnetic (at 1.0 A) component contains chiefly mafic rock-forming minerals and several types of secondary iron and manganese oxide minerals and amorphous mixtures, often referred to by the field term 'limonite." Differences in analytical values between the two fractions are mostly due to the mineralogical differences between them—though in some cases, minerals and metal values span the two fractions. Geochemical anomalies usually contain metal concentrations that result from both primary and secondary processes; these two fractions are valuable to understanding the contribution of each dispersion process. The primary ore-metal suite is usually represented in the nonmagnetic fraction because in metallized areas this fraction frequently contains heavy primary- and secondary-ore minerals. On the other hand, where there are deeply weathered, relict-hypogene (gossan) situations or where secondary metal dispersion has resulted in metal fixation by hydrous iron oxides (limonite) and manganese oxides of various types and origins, the metal suite deposited by or interacting with oxidizing solutions are selectively, though not exclusively, concentrated in the magnetic fraction.

ANALYTICAL METHODS

The prepared samples were analyzed by semiquantitative emission spectrography for 30 elements (Grimes and Marranzino, 1968). These spectrographic data are reported in parts per million on a scale with approximate geometric midpoints, such as 1,000, 700, 500, 300, 200, 150, and 100. The precision of these data is within one adjoining

[1]Any use of trade names is for descriptive purposes only and does not imply endorsement by the U.S. Geological Survey.

reporting interval 83 percent of the time and within two adjoining reporting intervals 96 percent of the time for all elements sought and for all materials tested (Motooka and Grimes, 1976). Only selected metals among the 30 scanned are discussed in this report. Some of the elements have low variation, were seldom detected, or have no obvious bearing on studies of metal deposits in the region, and therefore are not treated here. Analytical and statistical analyses for all of the elements have been reported earlier (Watts and others, 1978b).

DATA REDUCTION

All data were entered into the U.S. Geological Survey (USGS) computer data storage system entitled RASS (Rock Analysis Storage System). The data were then retrieved and analyzed statistically using USGS STATPAC programs (VanTrump and Miesch, 1977; Alminas and VanTrump, 1978; VanTrump and Alminas, 1978). Summary statistics derived from graphical analyses of log-transformed data were reported by Watts, Hassemer, Siems, and Nishi (1978b). Programs used here for data reduction and analysis include computer contouring (STPMAP), relative element magnitude (REM), and relative fraction magnitude (RFM).

The geochemical maps for each metal of interest (figs. 3–22) were computer plotted using the contour program STPMAP (VanTrump and Miesch, 1977). This program generated cell-averaged maps with intervals chosen within the anomalous population, thereby excluding areas considered background from within the contours. The contouring was based on a square grid 1.1 km on a side which required 42 cells in the east-west direction and 25 cells north-south in order to fit the unequal dimensions of the map area. With the dense sample-site distribution, the cell dimensions resulted in relatively unsmoothed contours, often with rather sharp curvatures that closely resemble contours based on the raw data.

After the cell size was established by computation, a circle of an appropriate search radius (1.7 km) calculated by the program was centered at each grid intersection. Then, the metal values within each circle were averaged and posted at the intersection. In order to achieve continuity of contour lines empty cells within sampled areas were assigned a default value. Finally, the parameters for these contour values were written on a plotting tape, which was used to generate mylar contour maps at a scale of 1:250,000 using a flatbed plotter. Large areas where no sampling was done were not contoured though inherent weaknesses in the gridding program have caused a slight shifting of contours into these areas.

GEOCHEMICAL HALOS

The most defined geochemical anomalies, both areally and in terms of anomaly to background contrast, are associated with eight general areas: Central mining district, Fierro-Hanover districts, Georgetown district, Pinos Altos district, Fleming Camp area, Chloride Flat-Boston Hill district, Juniper Hill area, and the adjacent vicinities to the north within Turkey Creek Canyon, Sycamore Creek, and Bear Creek. Of these eight areas, seven contain known mineral deposits, but the geochemical anomalies are not exclusively attributable to these sources. The Circle Mesa area may become a site of new mineral discoveries as with the other areas, but no deposits are presently known as opposed to the other areas.

There are other geochemically anomalous parts of the study area, but the anomalies are not as specifically localized nor in most cases, as intense; rather, they are generally pervasive occurrences of such lithophilic[2] elements as barium, manganese, and zinc (zinc is both lithophilic and chalcophilic), or scattered occurrences of such chalcophilic[3] metals as silver, copper, and lead. The anomalies north of lat 32°52'30"N and west of long 108°16'00"W in the volcanic terrane are of particular interest in this respect. The broadly blanketed enrichments of lithophilic elements are presumably fixed within the various amorphous and crystalline oxides of manganese and iron (magnetic fraction).

In order to account for this widespread enrichment of these elements, causative factors common to all the areas must be invoked. All the elements comprising this anomalous suite (chiefly Mn, Pb, Zn, and Ba) are readily available within the feldspars and mafic rock-forming minerals present in igneous host rocks. Because volcanism is a common denominator, it is here proposed as the dominant factor. The metals have probably been extracted from rock-forming minerals by alteration. Heated meteoric water of slightly acidic composition either convecting within a water-saturated volcanic pile or associated with plumes above subvolcanic intrusions could provide the mechanism of transportation; one which could be expected to be a common, if not a prevalent, characteristic of the volcanism. The solutions moreover would be oxidizing and would be capable of providing pervasive invasion of volcanic caprock and deposition of metals within oxide phases.

---

[2]Lithophilic elements form in the lithosphere or upper Earth's crust where they enter the lattice of silicate minerals.

[3]Chalcophilic elements have a strong affinity for sulfur and include a large number of the metals that form metallic ore deposits.

Where the chalcophilic elements are geochemically enriched within the volcanic terrane, mobilization and redistribution of metals from sulfide protore or Laramide ore deposits may have occurred. Metals may have also been introduced from magmatic emanations associated with subvolcanic intrusives. Anomalies of both chalcophilic and lithophilic elements of the felsic rock suite (Sn, Be, Nb, and Mo) could have these origins. Subvolcanic intrusives may also have caused local metal depletions as well as introductions, resulting in some of the geochemical lows seen on the maps.

Faults either provided conduits or exerted a control over the emplacement of intrusives in the volcanic terrane because there are close spatial associations between many of the geochemical trends and mapped faults (Finnell, 1976a, b; Moore, 1953).

The metal groupings used in the following discussion are based on geochemical similarities and on coextensive areal distributions as shown on the geochemical maps (figs. 3–22).

LEAD, COPPER, AND ZINC

Lead shows the broadest and best defined anomaly patterns (fig. 3). The anomalies are limited for the most part to the southern half of the study area where erosion reaches deeper stratigraphic levels. The nonmagnetic lead anomalies, being largely due to detrital ore minerals, indicate areas where primary mineral deposits are near the surface but may have undergone lateral mechanical transport for short distances. Because of the surface stability of most ore minerals of lead, the lead anomaly trends probably conform closely to pathways followed by primary, metalliferous solutions as viewed on the regional or district scale. The trends are rectilinear with dominantly northwest and northeast orientations. Known mineral deposits are at the intersections of several of these linear patterns; in such areas, the intersections are characterized by a broadening and intensification of the anomaly.

The areal distributions of lead associated with iron and manganese oxide phases (fig. 4) are less widespread than those related to the ore minerals (nonmagnetic fraction) because conditions favorable to these accumulations are more restricted. Controlling factors to the development of strong anomalies in the magnetic fraction include (1) high permeability of host rock to descending, oxidizing meteoric solutions, (2) chemical reactivity of host rock, and (3) abundance of pyrite. The conditions favorable to oxide-related lead anomalies prevail near the Mimbres and Barringer faults, and within the Groundhog fault trend, within areas parallel to the Silver City fault and near the north-

trending range front fault west of Juniper Hill. (See fig. 2.)

Copper is distributed over a much smaller area than is lead (fig. 5). The copper-dispersion patterns are similar in areal distribution to each other in both fractions, although they are somewhat displaced from each other locally (fig. 6). The nonmagnetic fraction contains most of the copper-ore minerals, where present, but certain copper-ore minerals are magnetic at 1.0 A; therefore, ore minerals can accumulate in either component. The Central and Pinos Altos districts contain most significant copper enrichments. The anomaly patterns in the Central district conform to the geologic structure and the trends of the known veins; whereas, those at Pinos Altos broadly replicate the shape of the intrusive stock. The anomaly patterns on the northwest side of the Fierro-Hanover stock show the influence of the Barringer fault—whether as a localizer or displacer of mineral deposits cannot be determined from the geochemical pattern conclusively. In the Georgetown silver district, copper and molybdenum (figs. 12, 13) are sufficiently enriched to suggest that economic concentrations of these metals may occur at depth below the silver zones. On the basis of the geochemistry, the Fleming Camp area would appear to have little copper at the surface. This may, however, be an effect of metal zonation in the vertical plane of the type shown at Pinos Altos (Hernon, 1953) rather than a measure of the amount introduced by metallization or removed by leaching. If base metal orebodies exist at depth as geochemical evidence suggests, copper content may increase with depth as it does at Pinos Altos (Hernon, 1953).

Zinc-producing districts are well outlined by the zinc geochemical patterns (fig. 7). The zinc-lead replacement deposits at Shingle Canyon are shown by the geochemical map to occur at the intersection of linear-shaped zinc contours that parallel the Mimbres and Barringer faults. In a similar manner, zinc geochemical patterns coincide with the Groundhog zone of faults, dikes, and zinc-producing mines. A well-developed northwest-trending zinc halo extends through the northern parts of the Pinos Altos stock and connects with an altered zone north of Juniper Hill and may well reflect a cogenetic relationship between the two areas. The zinc halo at Pinos Altos is similar in shape to the outcrop pattern of the stock, as it is with several other metals. This close spatial relationship indicates the closeness of genetic ties.

Zinc associated with oxides of manganese and iron and probably some marmatite (Fe-Mn-rich sphalerite) (fig. 8) is similar in geographic distribution to the nonmagnetic fraction within the mineral districts. Beyond the mining districts, though, similarities end. Areal distribution of magnetic-fraction anomalies is far more ex-

tensive. The anomalies continue beyond the perimeters of known deposits, particularly northward into the volcanic terrane. There is little disruption of these geochemical patterns even though they transect varying rock types and levels of stratigraphic exposure. One of the more prominent contour patterns broadly parallels the northwest-trending Mimbres fault, which past studies (Watts and others, 1978a) have shown is paralleled by coextensive anomalies of both zinc and manganese for a distance of about 29 km to the southeast from near Shingle Canyon. Apparently, zinc-manganese anomalies along significant structures peripheral to mining districts are common. Olade and Fletcher (1976) noted similar zinc-manganese concentrations within a fault zone adjacent to a major metal-producing district in British Columbia. The zinc-manganese enrichments were found in that case to be localized within the fault zone itself. They considered these metal concentrations to be mobilized and peripherally redistributed products of hydrothermally leached mafic minerals from within zones of intense alteration in the main mining district. Anomalies of zinc and manganese (figs. 8, 20) in the volcanics may be related to and mark the positioning of rock alteration and leaching at depth, or perhaps even the remobilization of deep-seated protore. If so, they are clues to deep exploration targets. The low area in the north-central part of the map area of figure 8 (shown by hachure) may be an area of zinc depletion, as it apparently is of manganese depletion also (fig. 20). This zone may indicate the position of a large, centered high-heat source—perhaps a buried intrusive body that has been instrumental in the mobilization and removal of metals. Another, less auspicious interpretation may be that the ash-flow tuff in the area has covered the zinc-manganese enriched zones subsequent to their deposition. These postulates require further investigation.

BISMUTH AND TUNGSTEN

Bismuth probably associated with bismuth sulphosalts and tungsten related to scheelite (figs. 9, 10) prominently characterize the areas of Pinos Altos and Fleming Camp. There is also bismuth at similar levels of concentration near the Barringer fault and on the contact-metamorphic margins of the Fierro-Hanover stock. The distribution of zinc in these same areas indicates that it may belong to, but is not restricted to this metal suite. The association bismuth-tungsten-zinc from empirical observations can be a guide to skarn-replacement mineralization in the Silver City region. At Pinos Altos, large tonnages of skarn-replacement zinc-copper-lead ore are present in the host rocks surrounding the Pinos Altos quartz monzonite

stock (McKnight and Fellows, 1978). At Fleming Camp, intrusive rock has not been mapped, yet the bismuth-tungsten-zinc anomalies are similar in intensity and in areal extent to those at Pinos Altos. The levels of concentration of the metals tungsten and bismuth indicate that they are dominant constituents of discrete mineral phases. Nonmagnetic, anomalous tungsten can be attributed to scheelite, which was identified in samples from both Fleming Camp and Pinos Altos. The minerals bismuthinite (Bi_2S_3), matildite ($AgBiS_2$), cosalite ($Pb_2Bi_2S_5$), and emplectite ($CuBiS_2$) were identified in veins at Pinos Altos (McKnight and Fellows, 1978). These minerals are typical of skarns and of high-temperature veins (Palache and others, 1952). Though these minerals were not observed in samples, either these or similar heavy minerals are believed to be present in alluvium derived from the Pinos Altos, Fleming Camp, and Fierro-Hanover districts.

Tungsten, as opposed to bismuth in any significant amounts, also occurs in the magnetic fraction. Although this component can contain wolframite-series minerals, they were not noted in the mineralogic scans; whereas, abundant limonite and hydrous manganese oxides were noted. Nearly all tungsten anomalies in the magnetic fraction occur at Fleming Camp and near Circle Mesa (fig. 11), which, perhaps of genetic significance, are also the only two areas where more than sparse amounts of detrital fluorite have been identified (Watts and Hassemer, 1980). The anomaly at Circle Mesa (northwest anomaly), which occurs in volcanic host rock, is associated with a zone of felsite intrusives, and minor base-metal anomalies, as well as the fluorite. The tungsten is thought to reside in manganese oxide minerals (possibly psilomelane), which are abundant in the area. (See fig. 20.) Tungsten is known to associate with certain types of manganiferous hot-spring deposits, such as those at Golconda, Nev. (Kerr, 1940). Kerr concluded that veins of hypogene tungsten minerals (presumably scheelite or wolframite-series minerals) are present in the subsurface somewhere along the circulation pathways followed by the heated meteoric water, and he concluded that tungsten was solubilized and extracted from these veins, transported upward, and coprecipitated with the oxide phases of manganese.

Scheelite is known to occur at Fleming Camp but not Circle Mesa. Some of the scheelite at Fleming Camp may be secondary in origin because, according to Rankama and Sahama (1950, p. 629), hydrated tungstic oxide is the usual stable phase in the weathering zone above primary tungsten ores, but if carbonate rocks are present, and calcium is available, tungstic oxide may go into solution as an alkalic tungstate and precipitate as secondary scheelite. The apparent

absence of scheelite at Circle Mesa may be related to the availability of calcium. Where calcium is unavailable to form scheelite during primary metallization, tungstic oxide may be fixed in hypogene manganese oxide minerals (Hewett and Fleischer, 1960, p. 25-28), which could be the origin of the anomalies at Circle Mesa. This does not rule out the possibility that scheelite may be encountered at depth at Circle Mesa.

Thus, tungsten occurrences at Circle Mesa and at Fleming Camp, in the magnetic fraction, can be attributed to a number of controlling factors. Weathering is probably a more significant contributor to the origin of the anomalies at Fleming Camp than at Circle Mesa, if the manganese oxides at Circle Mesa are hypogene in origin.

MOLYBDENUM

Molybdenum (fig. 12) is associated with lead, zinc, and copper and is most prominent at Fleming Camp, in the Central district, and at Georgetown. Strong molybdenum signatures occur where secondary base-metal-molybdenum deposits are present, because the associated minerals in these deposits are both heavy and surface stable. A large variety of vanadate, molybdate, and arsenate minerals can be expected in heavy-mineral samples within the mining region. Secondary, detrital ore minerals, such as wulfenite, account for most molybdenum anomalies with the highest anomaly to background contrast, which is for the most part an indication that the source deposits are highly oxidized, likely small, and near surface. The strong geochemical contrast shown by molybdenum and its excellent correlation with equally strong lead values near the southwest end of the Groundhog trend of faults, dikes, and mines in the Central district is probably related to the presence of wulfenite ($PbMoO_4$), which has been reported there by Lasky (1936, p. 78-79). Molybdenum-lead correlations elsewhere in the Silver City region indicate similar occurrences. The Georgetown district and areas southward along the Mimbres fault, and an area on the east-central margin of the map (east of Santa Rita copper deposit), are other examples.

In an oxidizing environment, molybdenum is mobilized as several molybdenum species in the acidic ore zone and then can be fixed in alkaline soil in the presence of coprecipitating iron hydroxides (Titley, 1964). Molybdenum concentrations in the magnetic fraction at Boston Hill probably result from the fixation of molybdenum in secondary iron-manganese oxide materials which in that area occur in abundance (fig. 13). Molybdenum fixed in this manner, in significant-

ly high concentrations, has not been encountered extensively in the study area as a whole, though the Tertiary volcanic rocks contain lesser, marginally anomalous amounts in places (particularly north of Pinos Altos). Molybdenum at these levels of concentration was eliminated by the computer averaging technique used in this study. The marginally anomalous data can be found in Watts, Hassemer, Siems, and Nishi (1978b).

SILVER AND GOLD

Silver and gold are somewhat similar in distribution on the anomaly maps (figs. 14, 15, 16), though silver is by far the most widespread, often occurring in association with such metals as lead and molybdenum, to the exclusion of gold. However, because of geochemical similarities between the metals, they are discussed together.

Surface-stable silver-bearing minerals of chiefly secondary origin account for most occurrences of anomalous silver in the nonmagnetic fraction. These heavy minerals are relatively immobile chemically in the near-surface environment, and they constitute the chief source of silver production (Hernon, 1953). Where these minerals are encrusted by transported limonite or are contained in the hydrous iron-manganese oxides within the weathered zone, lesser amounts of anomalous silver may be found in the magnetic fraction, which accounts for the similarities in geographic distributions of silver in the two fractions and for the far more limited extent of magnetic silver (fig. 15). The magnetic silver may be more concentrated in zones where associated primary minerals have a high iron content or in areas of high permeability, as may occur along the fault zones (for example, the Mimbres fault) because of more efficient weathering and oxidation.

Not unexpectedly, the principal areas outlined by gold contours are in the Pinos Altos district and at the known gold placer deposits near Bayard, N. Mex., in the Central mining district (Lasky, 1936). The Pinos Altos district contains the most prominent dispersion halo of gold, mostly within drainage areas within the stock itself. This gold is in the native state as detrital grains in the alluvium derived from the Pinos Altos stock.

The gold anomalies indicate the amount of gold detected by emission spectrography, which is an imprecise method for analyzing gold. In some cases, the analyses do not show areas where gold was visually identified in concentrated sediments. The anomalies reflect the amount of gold detected where 4-5 kg of bulk samples were reduced

by panning and other processing to nearly one-thousandth of its original size. Because this gold is both particulate and malleable, it was sometimes missed by the analyses. Therefore, when coherent anomaly patterns can be produced from the analyses, gold must be very abundant in the associated drainage basins, because sparse, scattered detrital grains would produce scattered, erratic geochemical anomalies.

In addition, the geochemical method cannot be used to evaluate grade and tonnage of particulate gold; this evaluation requires special techniques of placer study in which the volume of alluvial material containing a given quantity of gold is estimated. The geochemical method only locates the gold occurrences and identifies areas where gold is most abundant.

Gold may also be used as a pathfinder to other types of deposits. Gold is a characteristic metal of the mineralization at Pinos Altos (fig. 16). Because of geochemical similarities between Pinos Altos and Fleming Camp, it was earlier postulated that copper content at Fleming Camp may increase with depth as it does at Pinos Altos (Hernon, 1953); as a corollary, gold content may also increase with depth.

BARIUM AND MANGANESE

Neuerburg, Barton, Watterson, and Welsch (1978) have observed that the lithophilic elements barium and manganese, in addition to iron, silica, and zinc, are redistributed during the alteration of rocks and are ultimately deposited in the gangue minerals and on the periphery of metalliferous deposits. Olade and Fletcher (1976) have made similar observations, which they attributed to acid-hydrothermal leaching along an advancing replacement front as envisioned by Korzhinskii (1968). These observations suggest that manganese and barium can provide important clues to patterns of alteration brought about during regional metallization. The similarity of zinc contours to those of manganese has been discussed; the geochemical maps show that these distributions are similar for barium as well.

The barium map of the nonmagnetic fraction (fig. 17) is also a barite map because, at high concentrations, the metal content is due to the presence of that mineral. Barite is the most common mineral of barium; it is a gangue mineral in metal deposits and an additive alteration product, and it is the least soluble and most common alkaline-earth sulfate associated with hydrothermal systems (Neuerburg and others, 1978; Holland and Malinin, 1979, p. 495). During hydrothermal leaching, barium can be derived from potassium-

feldspar within the host rocks. Because of the prograde characteristics of barium in solution, Holland and Malinin (1979, p. 498, 499) believed that simple cooling is sufficient to account for the precipitation of barite from solution, although other factors must still be considered. These conditions presumably can exist in highly fractured areas and near the surface. Because barite forms around and above metal deposits, knowledge of the positioning of these barite halos can be useful in locating covered deposits. The north-northeast-trending contours indicate barite-enrichment zones that may be either peripheral to or coextensive with the surface trace of ore-solution conduits. Interpretations of the significance of the barite halos can be complicated by considerations of the erosion level. For example, the continuous, north-northeast-trending contour patterns link some of the mineral districts to each other, and because erosion is rather deep within the mining districts (south of lat 32°52'30" N.), these barite halos may be on the lateral periphery of potential zones of mineral deposition or of alteration because preexisting overlying halos may be eroded away. In volcanic terrane north of lat 32°52'30" N., however, the halos may be vertically above altered zones or solution conduits on account of erosional stripping being much less.

Most barium in the magnetic component (fig. 18) is probably associated with several types of hydrous manganese oxides in which barium is held as a coprecipitated or adsorbed constituent (Levinson, 1974); or in the case of crystalline minerals, it is part of the structure (for example, the case of the mineral hollandite). This association is well documented in the literature and can be seen here by comparing the manganese and barium geochemical maps (figs. 18, 20). The usefulness of barium-rich, secondary manganese oxides in exploration is yet to be determined, but hydrothermal alteration and mineralization may cause these concentrations of barium in association with hydrous manganese oxides at the lateral or vertical periphery of metal deposits. Surface weathering of preexisting rock-forming minerals can also cause these concentrations as well, which suggests that any interpretations of manganese-barium anomalies should also consider the intensity of the weathering environment.

The manganese distribution in figure 19 shows where nonmagnetic, generally primary manganese minerals, such as manganiferous carbonates, are most concentrated. Because most primary gangue minerals are deposited in veins during the metallization events, though mostly on the vertical or lateral periphery of the main chalcophilic orebodies, the distribution of minerals of this kind can be of interest in exploration. Where weathered, most of these minerals convert to secondary hydrous manganese oxides, which are ultimately surface stable; in the Chloride Flat-Boston Hill district

manganiferous mesitite ($FeMgCO_3$) was considered to be the primary progenitor of the secondary manganiferous iron-ore deposits (Entwhistle, 1944). Figure 20 shows extensive areas within the mineralized districts where minerals of this type are presumably in abundance. Outside the known metallized areas, as for example, near Circle Mesa and several kilometers north of Fierro near Skate Canyon (both within volcanic terrane), extensive areas with anomalous nonmagnetic manganese have been detected in the sampling. Presumably, these zones reflect the presence of primary, nonmagnetic vein minerals of manganese (probably carbonates). These occurrences may indicate the replacement and mobilization of carbonate from Paleozoic rocks beneath the volcanics. Replacement of the Paleozoic rocks may have also involved metallization.

Manganese displays pervasive and complex patterns of distribution in the magnetic component. These patterns are not unexpected because figure 20 depicts the distribution of hydrous manganese oxides, which are exceedingly widespread and may have several origins, and are selectively fractionated into the magnetic heavy-mineral component. The oxides of manganese present within the mineral districts are probably derived from the supergene weathering of preexisting primary manganiferous minerals, particularly vein and replacement deposits of manganiferous carbonate. Two prominent areas where this may be the case are at Boston Hill where manganese-iron deposits are now being mined, and along the Barringer fault where, as reported by Hernon, Jones, and Moore (1953), manganese replacement deposits are found in adjacent wallrock.

The apparently pervasive distribution of manganese oxides within the areas covered by middle Tertiary volcanics suggests that volcanism may have contributed to these concentrations. Heated meteoric water within a water-saturated, tuffaceous volcanic pile could have provided the mechanism that allowed manganese to be leached from the host rocks within the pile at depth and to be transported upward to sites of deposition. In fact, hot-spring and apron deposits of primary manganese oxide minerals are rather common occurrences in volcanic areas (Hewett and Fleischer, 1960). Because the anomaly trends of manganese and the geologic trends coincide somewhat and because the anomaly patterns transect the minor climatic differences that exist between the northern and southern parts of the area (Trauger, 1972), weathering alone probably is not the most significant determining factor leading to enrichment in the bedrock of these manganese oxides. On the other hand, when the manganese anomaly map and the geology are compared, faults appear to be a controlling influence on the concentrations—either in the localization of the primary minerals during deposition or in the

promotion of their later oxidation, and thus strong residual concentration, or both.

TIN

Tin (fig. 21) appears to have been introduced during metallization in the Silver City mining region. Anomalies of nonmagnetic tin occur at Fleming Camp, Pinos Altos, Central district, Georgetown, Circle Mesa, and near the Silver City stock. Heretofore, tin has not been recognized as a metal component of these ores; although present, it is unlikely to be in economic amounts. The mineralogic source of the tin has not been determined, though elsewhere in the region anomalies of about 700 parts per million or more can be attributed to the presence of cassiterite (SnO_2).

VANADIUM

Vanadium values in the nonmagnetic component at high levels of concentration are a result of discrete, vanadium-bearing ore minerals, chiefly secondary in origin, that occur in the supergene zone of oxidizing lead-zinc vein deposits. Vanadinite (lead vanadate) is the most common mineral of this type. Figure 22 shows the distribution of these secondary vanadium-bearing ore minerals. Vanadinite has been identified at Georgetown (Lasky and Wooten, 1933, p. 57), and an arsenic-rich variety of similar appearance, endlichite $Pb_5(V,AsO_4)_3Cl$ in association with cuprodescloizite (mottramite) $((Pb,Zn,Cu)_3(VO_4)_2 \cdot (Pb,Zn,Cu)(OH)_2)$, was identified at the Lucky Bill mine in the Central district (Lasky, 1936, p. 84). Areas where the geochemical maps suggest the presence of these minerals are (1) about 4–5 km east of Santa Rita porphyry copper deposit, (2) near the Mimbres fault and at Georgetown, (3) west of Pinos Altos, and (4) the Central district.

INTERPRETATION

SELECTION AND DESCRIPTION OF WINDOW AREAS

The characteristics of the geochemical anomalies were compared quantitatively between several geographic areas that were selected on the basis of anomaly clustering (figs. 3–22). The boundaries of each anomaly cluster were blocked off geographically on the basis of maximum spread of a discrete cluster of anomalous values, though

somewhat arbitrarily, and held constant. The anomaly characteristics were calculated on metal values in the anomalous range, and the assumed threshold values remained the same for both fractions and in all window areas. Locations and descriptions of the selected window areas are shown in table 1.

COMPARISON OF HEAVY-MINERAL FRACTIONS

The U.S. Geological Survey STATPAC program relative fraction magnitude (RFM) (Alminas and VanTrump, 1978) was used to compare anomalous metal contents between heavy-mineral fractions in each of the areas. The fractions are compared on the basis of two factors: halo intensity and halo size. The product of these two factors is the fraction magnitude (FM), which is calculated for each of the selected metals separately within each window area. The information from these comparisons can be used to assess the relative influence of weathering, and perhaps resultant supergene dispersion in each area on any selected metal, but it mainly applies to those metals considered to be chalcophilic. This is a method of determining the degree to which the chalcophilic elements are retained by fixation within hydrous iron-manganese oxides through such mechanisms as adsorption and coprecipitation. The ratio FM (magnetic)/FM (nonmagnetic) provides an index that can be used for this purpose. Values for this ratio within each of the window areas are shown in table 2.

Table 2 shows that the degree to which the chalcophilic elements are associated with secondary iron-manganese oxides is in the decreasing sequence Zn-Cu-Pb-Bi-Mo-Ag. This sequence is obtained by summing the ratios shown in table 2 for each chalcophilic element; the lowest ratio sums occur for those elements on the right side of the sequence. This is also the sequence, excluding a close but reverse positioning of bismuth-molybdenum, of decreasing crustal abundance—zinc is the most abundant metal of the group in the crust, and silver is the least abundant (Krauskopf, 1967, p. 639–640). However, as stated by Rankama and Sahama (1950, p. 13), the nature of the products formed in hypogene and supergene reactions is dependent upon elemental abundance and is ultimately controlled by the law of mass action, which is also dependent on rate of dissolution. Therefore, concentrations of metal available and rate of dissolution of primary mineral species may account for the sequence. The sequence that developed from the ratios can be interpreted in the following manner: Elements such as bismuth and silver, which appear on the right or decreasing end of the sequence, occur in the most surface-stable, secondary- or primary-ore minerals and are weakly mobile in

supergene solutions—assuming iron and manganese are present and secondary iron or manganese minerals or amorphous aggregates are allowed to form. Where only a nonmagnetic component appears, the primary progenitors may have been iron-free sulfides and sulfosalts.

The sums of FM ratios for the chalcophilic elements silver, bismuth, copper, molybdenum[4], lead, and zinc were compared between window areas, and a sequence of the areas was derived. This sequence indicates a decreasing association of the selected metals with the secondary iron and manganese oxides, and, indirectly perhaps, with oxidizing, primary or secondary solutions. The sequence is (1) Skate Canyon (Sheep Corral Canyon), (2) Circle Mesa, (3) Chloride Flat-Boston Hill district, (4) Fleming Camp area, (5) Pinos Altos district, (6) Shingle Canyon district, (7) Fierro-Hanover district, (8) Juniper Hill district, (9) Georgetown district, and (10) Central district. Interpretations of this sequence are complicated by the fact that Skate Canyon, Sheep Corral Canyon, and Circle Mesa may contain anomalies derived from ascending, heated, oxidizing meteoric waters; whereas, the others may result from cooled, descending (supergene) waters. Given the type of data used in this report, a definite distinction is not possible.

COMPARISON OF GEOCHEMICAL HALOS

The computer program element magnitude (EM) (VanTrump and Alminas, 1978) was used to compare halo characteristics between the anomalous areas (table 3). The values calculated by this program are similar in most respects to the linear productivity measurement (Beus and Grigorian, 1977, p. 94). The linear productivity is a measure of the size and intensity of the primary metal halo surrounding an orebody at a given vertical level. This measurement, which is expressed in meter-percent, is the product of the average anomalous value and the maximum lateral distance from the orebody. Compared at different vertical levels, the measurement provides both an index of metal zonation in the vertical plane and a quantitative method of comparing different metal deposits as to type and relative relationship to the surface on the basis of vertical metal zoning. The nonmagnetic heavy-mineral fraction contains the ore minerals that

[4]Molybdenum is considered lithophilic in the upper lithosphere, but it also has a strong affinity for sulfur (Rankama and Sahama, 1950, p. 626-627). It is here considered with the chalcophilic elements because it forms the sulfide very readily.

characterize the metallization at or near the level of erosion represented by the present land surface. This sample medium differs from metal values obtained through partial (enhanced) metal extractions from rock samples derived from surface outcrops, which is the more common method of studying metal halos around mineral deposits (Beus and Grigorian, 1977, p. 78–90), only in that the ore-related metals contained in an alluvial heavy-mineral concentrate have been transported short distances as part of the mechanical stream-sediment load. This potential shortcoming in the method is mitigated somewhat by the fact that in most areas, particularly where known deposits or alteration exists, small drainage systems were sampled and the distances from the source outcrop are short. The heavy-mineral technique employed in this report should work well as a sensitive indicator of metal zonation because the enhancement of the ratio of anomaly to background contrast, as achieved by the heavy-mineral method, can increase the depth range to which covered mineral deposits can be detected by as much as 1.5 times (Beus and Grigorian, 1977, p. 154), in addition to broadening the target area. This increased sensitivity to metalized areas makes it possible to investigate subtleties of metal dispersion and in some cases to study metals that due to low analytical sensitivity would be inaccessible to studies of metal zoning.

The EM measurement is a product of the element intensity, which is the ratio of anomaly mean to threshold and the areal size of the anomaly at constant threshold or lower limit of anomalous values. The theory and use of the method are further described in VanTrump and Alminas (1978). The method was conceived by H. V. Alminas of the U.S. Geological Survey. The EM measurement involves an areal measurement rather than a linear one, which is an advantage when ore-deposit centers are not known and drill data are not available. The area (shown in table 3) is a percentage value, proportional to the number of anomalous samples relative to those that are in background concentrations within the blocked-out window. Assuming a relatively uniform sample density, areal size (in m^2 or km^2) can be estimated by the product of sample density (m^2 or km^2/sample) and percentage value in table 3. Because sample density was not everywhere uniform, the areal size would not be realistic in the present study. The percentage value allows relative comparisons between areas without regard to sample density, assuming it is sufficient to characterize each area.

Table 3 shows the EM values for the windows, which are ranked in a decreasing sequence based on the product areal size and anomaly to background contrast (intensity).

RELATIVE EXPOSURE LEVEL

In areas of variable erosion, mineralized zones may be exposed through a wide vertical range. Within the Silver City mining region there are probably some metal deposits which are exposed near their roots that consist of minable deposits that crop out but do not continue at depth; other deposits may be exposed near the midpoint of the productive ore zone and consist of minable deposits that may extend to moderate depth. Still other deposits may be only peripherally exposed and will be characterized by metal anomalies of the supraore (peripheral) metal suite which in some cases may even be related to small ore deposits of these metals. The peripheral metal suite would include such metals as lead, silver, barium, antimony, and others. In extreme instances, metal deposits may be buried to such a great depth that they are beyond the depth range or distal detection limit of the geochemical method. We attempted to assess these erosional factors within the study area.

The comparisons made here are based on a simple model of metal zonation, which based on characteristics of the known mines, the geology and distribution patterns of the geochemical anomalies, seems to fit the Silver City mining region. In most metalliferous deposits that contain the metals lead, barium, and silver within a primary halo, dispersion patterns characteristically expand laterally and rise vertically above main orebody level; whereas, the primary dispersion patterns for the metals copper, molybdenum, and bismuth expand laterally at and below vertical level of the orebody until the roots are reached, at which point all metals wedge out. The metal suites characterizing these positions in the vertical zoning of metal dispersion are termed supraore and subore, respectively, in the usage of Beus and Grigorian (1977). Where the dispersed metals are also the ore metals sought, maximum halo size (lateral distance) and greatest metal enrichment are usually at the orebody level (Beus and Grigorian, 1977, p. 155). For example, at several stockwork molybdenum deposits, certain metals form typical enveloping halos, and the metal dispersion is zoned about the main ore zones (Wallace and others, 1978; Sharp, 1978). Sharp (1978, p. 373-376) showed drilled cross sections at a breccia pipe complex in Redwell Basin, Colo., in which a broad, primary lead halo at the surface wedges out 300-500 m above the main molybdenum orebody; a broad, primary zinc aureole occurs at the surface and terminates above the molybdenum orebody, and a tungsten halo occurs immediately above and overlaps the molybdenum orebody where maximum molybdenum dispersion occurs. Metal zonation is a common feature of most economic mineral

deposits; it is not characteristic of dispersed subeconomic metal anomalies (Beus and Grigorian, 1977, p. 134–147).

The amount of erosional exposure relative to several known or potential inner ore zones was assessed using element magnitude (EM) calculations for selected metals within the window areas. Calculations are based on the assumption that those halos dominated by the supraore metal suite are peripheral to or above the center of the metal zonation sequence; whereas, the subore suite is closer to the center of the metal system. The metal system model is simple and general but should embrace a variety of large deposit types, mostly related to igneous activity. The metals assumed to be peripherally dispersed (supraore) are lead, silver, and barium, and those assumed to be near to or within the inner metal zone are copper, molybdenum, and bismuth. The selection of metals was based on descriptions of the known deposits in the region and the documented behavior of these metals in an environment of hydrothermal mineralization and alteration elsewhere in the world. (See for example Beus and Grigorian, 1977.) The additive element magnitudes (EM) of the peripherally dispersed metals (supraore) were then ratioed to the subore suite as shown in table 4.

Table 4 shows a sequence whereby the window areas are ranked in order of decreasing ratio sum, which is believed to indicate an order of increasing depth of surface exposure due to erosion of the known or postulated inner metal zone (center of the metal system) within each of the areas. From the table, the least exposed deposits are in the Georgetown district and at Fleming Camp, which suggests that ore of the subore suite may be discovered at depth in these areas and that the silver produced in these two districts is supraore or peripheral. The calculations indicate also that the Fierro-Hanover district is eroded to a level of exposure that may be close to the roots of the main, inner metal zone, but the erosional level is not as deep in a southwestward direction toward the Central district, possibly because of a southwestward plunge of the ore zones. To check the validity of these experimental conclusions requires further assessment through more detailed investigations, including physical exploration, particularly at depth within the areas indicated to have high ratios.

CONCLUSIONS

The geochemical maps show that several relatively unexplored targets still exist within the Silver City mining region. Possibly foremost among these targets is that near Fleming Camp. Because

the geochemical signature at Fleming Camp is similar to that of the skarn metalization at Pinos Altos, an intrusive body or cupola may be beneath the area at shallow depth.

Other targets of interest include the following: (1) The Georgetown district, where molybdenum and copper halos are strong enough to suggest the presence of these metals at depth, especially because these subore metals, though enriched at surface level, are subordinate in enrichment to metals of the supraore suite. (2) The Pinos Altos district, where the surrounding metalized zone appears more extensive than was previously realized. Additional deposits may exist at a greater distance from the contact zone, particularly to the northwest and southeast. (3) The vicinity of Circle Mesa, where a deep exploration target, similar perhaps to the one at Fleming Camp, may exist. The presence of tungsten suggests that intrusive-related skarn or stockwork deposits may be present at depth. Intrusive bodies occur within the volcanic tuff units of this area, possibly these are cupolas of a larger intrusive body at depth. The geochemical signature suggests that heated meteoric water may have caused the anomalies. (4) Along both the Barringer and Mimbres fault zones, where metalization appears extensive and suggests the possibility of deposits at depth in association with these loci. (5) The Juniper Hill area, which contains geochemical anomalies of unknown significance. The lead and zinc distributions indicate that metallization may be closely related to the mineralized areas at Pinos Altos and may in fact be a weakly mineralized extension. If mineral deposits do exist, the exposure-level calculations indicate that erosion has not reached root levels. The altered sills in the area may have entrapped ore beneath them. (6) The Sheep Corral Canyon anomaly, the significance of which is unknown. The presence of sparse amounts of bismuth and other metals is encouraging, but more data are required to prove this area to be a deep exploration target. A large quartz vein was noted near the head of a drainage within the center of the area. This quartz vein may be the result of the remobilization of silica from depth as a consequence of host-rock alteration or replacement. (7) Skate Canyon, where the geochemical anomalies suggest past hot-spring activity and mobilization of carbonate from depth, possibly as a result of host-rock replacement. Though not shown on a map, but indicated in table 3, the area contains strong magnesium anomalies as well, which strengthens the case for replacement of Paleozoic rocks at depth, particularly if they happen to be dolomitic.

The regional distribution of barium, zinc, and manganese presumably as hydrothermal halos is of particular interest because of the peripheral positioning of these metals to mineral districts and the possible usefulness of this relationship in exploration. The pro-

minence of these halos in the volcanic terrane suggests a genetic relationship to the volcanism. The distribution of barium (barite) in the nonmagnetic fraction may indicate the lateral periphery of metallized zones and ore-solution conduits in the more eroded terrane of the Silver City region and the top of the vertical metal zonation in the middle Tertiary volcanic terrane. The area north of Fierro and Georgetown contains a barium (barite) halo interpreted to be a product of mobilization and redeposition from hydrothermal alteration at depth.

The erosion-level interpretations are experimental and are subject to numerous unseen factors that could affect conclusions. Although the results compare favorably with known geologic relationships, the actual metal concentrations and zonal relationships at depth are obviously unknown. Comparison of metal zonation between different areas may be a method whereby the most promising targets in a group of several regional- or district-scale geochemical anomalies can be selected for further investigation, according to sequential priorities. Some assumptions may not be valid for all deposits in the region and there have out of necessity been simplifications, but the purpose is to glean the maximum information from geochemical data where there is no knowledge of the subsurface or where a geochemical anomaly does in fact indicate a buried deposit. Analogy is one way of approaching the interpretation.

REFERENCES CITED

Alminas, H. V., and VanTrump, George, Jr., 1978, Relative fraction magnitude program explanation and computer program listing: U.S. Geological Survey Open-File Report 78-1013, 23 p.

Beus, A. A., and Grigorian, S. V., 1977, Geochemical exploration methods for mineral deposits: Willmette, Ill., Applied Publishing Ltd., 287 p.

Cunningham, J. E., 1974, Geologic map and sections of the Silver City quadrangle, New Mexico: New Mexico Bureau of Mines and Mineral Resources Geologic Map 30, scale 1:24,000.

Entwhistle, L. P., 1944, Manganiferous iron-ore deposits near Silver City, New Mexico: New Mexico Bureau of Mines and Mineral Resources Bulletin 19, 72 p.

Finnell, T. L., 1976a, Geologic map of the Twin Sisters quadrangle, Grant County, New Mexico: U.S. Geological Survey Miscellaneous Field Studies Map MF-779, scale 1:24,000.

_____1976b, Geologic map of the Reading Mountain quadrangle, Grant County, New Mexico: U.S. Geological Survey Miscellaneous Field Studies Map MF-800, scale 1:24,000.

Grimes, D. J., and Marranzino, A. P., 1968, Direct-current arc and alternating-current spark emission spectrographic field methods for the semiquantitative analysis of geologic materials: U.S. Geological Survey Circular 591, 6 p.

Hawkes, H. E., and Webb, J. S., 1962, Geochemistry in mineral exploration: New York, Harper and Row, 415 p.

Hernon, R. M., 1953, Summary of smaller mining districts in the Silver City region, New Mexico, *in* New Mexico Geological Society Guidebook, 4th Field Conference, Southwestern New Mexico, p. 138-140.

Hernon, R. M., Jones, W. R., and Moore, S. L., 1953, Some geological features of the Santa Rita quadrangle, New Mexico, *in* New Mexico Geological Society Guidebook, 4th Field Conference, Southwestern New Mexico, p. 117-130.

Hewett, D. F., and Fleischer, Michael, 1960, Deposits of the manganese oxides: Economic Geology, v. 55, no. 1, 55 p.

Holland, Heinrich D., and Malinin, Sergey D., 1979, The solubility and occurrence of non-ore minerals, *in* H. L. Barnes, ed., Geochemistry of hydrothermal ore deposits [2d ed.]: New York, John Wiley and Sons, p. 495-500.

Jones, W. R., and Hernon, R. M., 1973, Ore deposits and rock alteration of the Santa Rita quadrangle, Grant County, New Mexico: National Technical Information Service Report PB-214-371, 102 p.

Jones, W. R., Hernon, R. M., and Moore, S. L., 1967, General geology of the Santa Rita quadrangle, Grant County, New Mexico: U.S. Geological Survey Professional Paper 555, 144 p.

Jones, W. R., Hernon, R. M., and Pratt, W. P., 1961, Geologic events culminating in primary metallization in the Central mining district, Grant County, New Mexico: U.S. Geological Survey Professional Paper 424-C, p. 11-16.

Jones, W. R., Moore, S. L., and Pratt, W. P., 1970, Geologic map of the Fort Bayard quadrangle, Grant County, New Mexico: U.S. Geological Survey Geologic Quadrangle Map 865, scale 1:24,000.

Kelly, W. C., 1958, Topical study of lead-zinc gossans: New Mexico Bureau of Mines and Mineral Resources Bulletin 46, 80 p.

Kerr, P. F., 1940, Tungsten-bearing manganese deposit at Golconda, Nevada: Geological Society of America Bulletin, v. 5l, p. 1359-1389.

Korzhinskii, D. S., 1968, The theory of metasomatic zoning: Mineralium Deposita, v. 3, p. 222-231.

Krauskopf, Konrad B., 1967, Introduction to geochemistry: New York, McGraw-Hill, 721 p.

Lasky, S. G., and Wooten, T. P., 1933, The metal resources of New Mexico and their economic features: New Mexico Bureau of Mines and Mineral Resources Bulletin 7, 178 p.

Lasky, S. G., 1936, Geology and ore deposits of the Bayard area, Central mining district, New Mexico: U.S. Geological Survey Bulletin 870, 144 p.

Levinson, A. A., 1974, Introduction to exploration geochemistry: Calgary, Alberta, Canada, Applied Publishing Company, Ltd., 612 p.

McKnight, J. F., and Fellows, M. L., 1978, Silicate mineral assemblage and their relationship to sulfide mineralization, Pinos Altos mineral deposit, New Mexico: Arizona Geological Society Digest, v. 1, p. 1-8.

Moore, S. L., 1953, Preliminary geologic map of the Allie Canyon quadrangle, Grant County, New Mexico: U.S. Geological Survey Open-File Report, 2 sheets, scale 1:24,000.

Motooka, J. M., and Grimes, D. J., 1976, Analytical precision of one-sixth order semiquantitative spectrographic analysis: U.S. Geological Survey Circular 738, 25 p.

Neuerburg, G. J., Barton, H. N., Watterson, J. R., and Welsch, E. P., 1978, A comparison of rock and soil samples for geochemical mapping of two porphyry metal systems in Colorado: U.S. Geological Survey Open-File Report 78-383, 26 p.

Olade, M. A., and Fletcher, W. K., 1976, Trace-element geochemistry of the Highland Valley and Guichon Creek batholith in relation to porphyry copper mineralization: Economic Geology, v. 71, no. 4, p. 733-748.

Paige, Sidney, 1916, Description of the Silver City quadrangle, New Mexico: U.S. Geological Survey Atlas, Folio 199, 19 p.

Palache, Charles, Bermon, Harry, and Frondel, Clifford, 1952, Dana's system of mineralogy [7th ed.]: New York, John Wiley and Sons, p. 275, 429-445.

Rankama, Kalervo, and Sahama, T. G., 1950, Geochemistry [1st ed.]: Chicago and London, University of Chicago Press, p. 13, 68, 626, 627, 629.

Schmitt, H. A., 1939, The Pewabic Mine: Geological Society of America Bulletin v. 50, no. 5, p. 777-818.

Sharp, J. E., 1978, A molybdenum mineralized breccia pipe complex, Redwell Basin, Colorado: Economic Geology, v. 73, no. 3, p. 373-376.

Titley, S. R., 1964, Some behavioral aspects of molybdenum in the supergene environment: American Institute of Mining and Metallurgical Petroleum Engineers Transactions, v. 299, p. 199-204.

Trauger, F. D., 1972, Water resources and general geology of Grant County, New Mexico: New Mexico Bureau of Mines and Mineral Resources Hydrologic Report 2, 211 p.

VanTrump, George, Jr., and Alminas, H. V., 1978, Relative Element Magnitude program explanation and computer program listing: U.S. Geological Survey Open-File Report 78-1014, 23 p.

VanTrump, George, Jr., and Miesch, A. T., 1977, The U.S. Geological Survey RASS-STATPAC system for management and statistical reduction of geochemical data, *in* Computers in Geoscience, v. 3: Oxford, Pergamon Press, p. 475-488.

Wallace, S. R., Mackenzie, W. B., Blair, R. G., and Muncaster, N. K., 1978, Geology of the Urad and Henderson molybdenite deposits, Clear Creek County, Colorado, *with a section on* a comparison of these deposits with those of Climax, Colorado: Economic Geology, v. 73, no. 3, p. 325-367.

Watts, K. C., and Hassemer, J. R., 1980, Distribution and abundance of fluorite in stream-sediment concentrates, Silver City 1° × 2° quadrangle, New Mexico and Arizona, U.S. Geological Survey Miscellaneous Field Studies Map MF-1183C, scale 1:250,000.

Watts, K. C., Hassemer, J. R., and Nishi, J. M., 1978a, Eastern Santa Rita quadrangle and western margin of Mimbres Valley, New Mexico: Journal of Geochemical Exploration, v. 9, no. 2/3, p. 175-186.

Watts, K. C., Hassemer, J. R., Siems, D. F., and Nishi, J. M., 1978b, A statistical summary and listing of the spectrographic analyses of heavy-mineral concentrates and conventional, sieved stream-sediment samples, Silver City area, New Mexico: U.S. Geological Survey Open-File Report 78-801, 247 p.

FIGURES 3–22,

TABLES 1–4

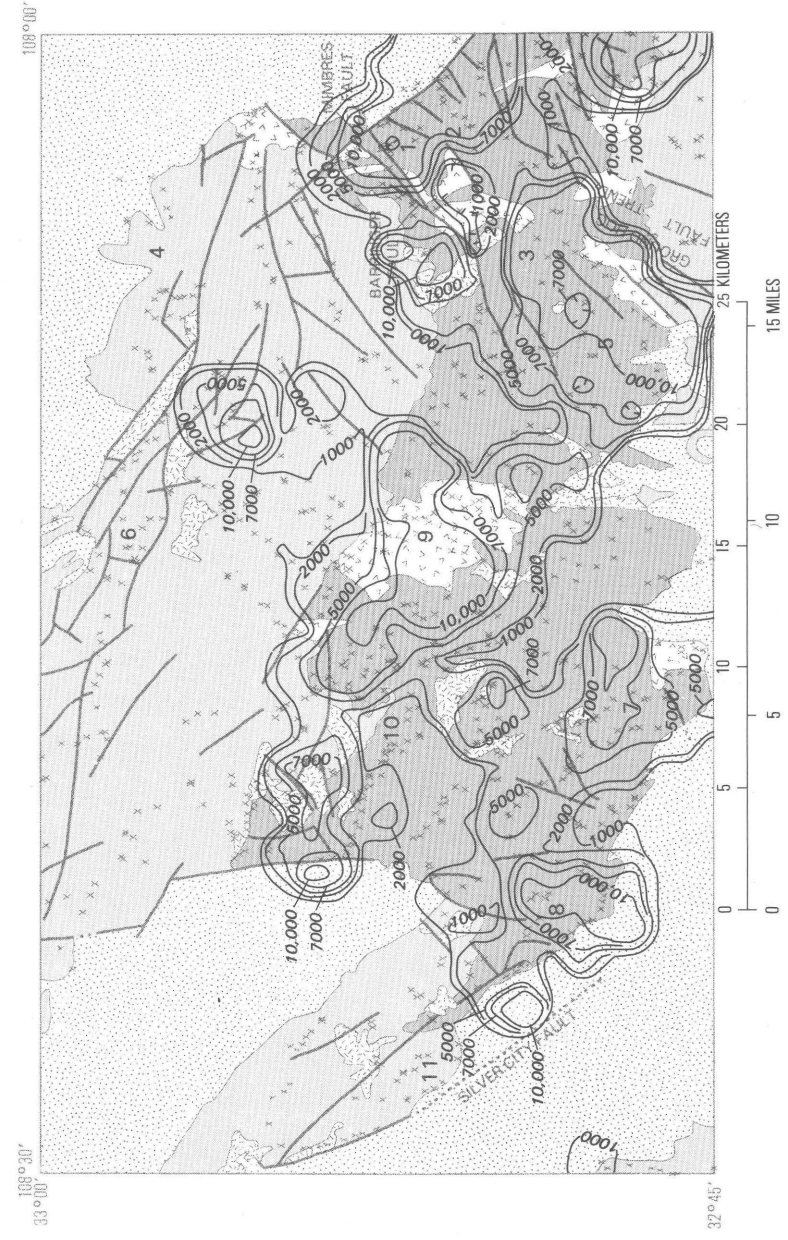
108°00'
33°00'
108°30'
32°45'
CAMBRES FAULT
BAR
GRO
FAULT
TRENC
SILVER CITY FAULT
0
5
10
15
20
25 KILOMETERS
0
5
10
15 MILES

EXPLANATION

QUATERNARY-TERTIARY BASIN-FILL SEDIMENTS AND PEDIMENT GRAVELS

MID-TERTIARY VOLCANICS

MID-TERTIARY INTRUSIVES

TERTIARY-CRETACEOUS INTRUSIVES

MESOZOIC-PALEOZOIC ROCKS—Includes small areas of Precambrian rocks

CONTACT

NORMAL FAULT—Dotted where concealed

SAMPLE SITE

3 MINING DISTRICTS AND OTHER GEOCHEMICAL ANOMALIES

1. Shingle Canyon district
2. Georgetown district
3. Fierro-Hanover district
4. Skate Canyon area
5. Central district
6. Sheep Corral Canyon area
7. Chloride Flat–Boston Hill districts
8. Fleming Camp area
9. Pinos Altos district
10. Juniper Hill area
11. Circle Mesa area

FIGURE 3.—Distribution of lead in the nonmagnetic fraction. Contours drawn at 1,000, 2,000, 5,000, 7,000, and 10,000 parts per million; hachures indicate closed areas of lower values. In some places, contours are shifted as much as 1.1 km (one grid cell) from sample localities due to computer averaging technique.

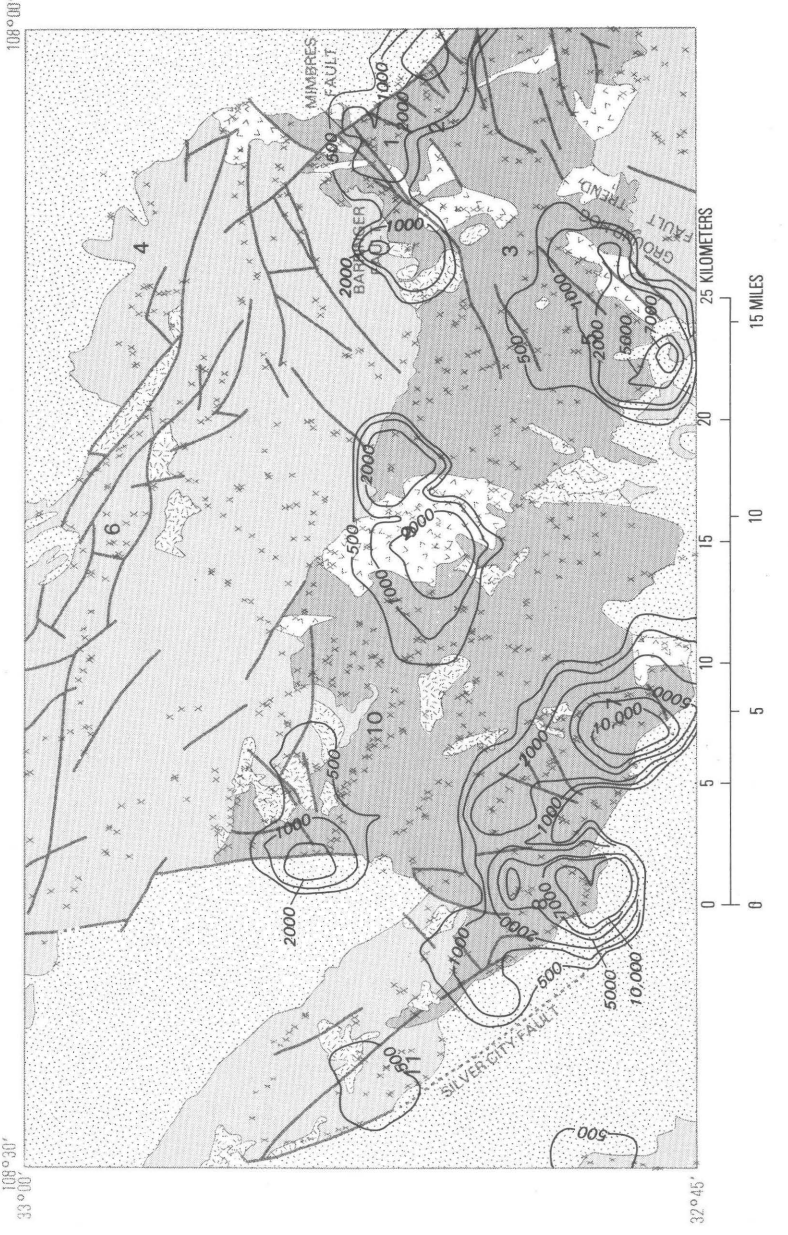
108°00'
33°00'
109°30'
32°45'
MIMBRES FAULT
BAYARD TREND
GROUNDHOG FAULT TREND
SILVER CITY FAULT
4
6
10
11
3
500
1000
2000
5000
10,000
0
5
10
15
20
25 KILOMETERS
0
15 MILES

EXPLANATION

QUATERNARY-TERTIARY BASIN-FILL SEDIMENTS AND PEDIMENT GRAVELS

MID-TERTIARY VOLCANICS

MID-TERTIARY INTRUSIVES

TERTIARY-CRETACEOUS INTRUSIVES

MESOZOIC-PALEOZOIC ROCKS—Includes small areas of Precambrian rocks

CONTACT

NORMAL FAULT—Dotted where concealed

SAMPLE SITE

3 MINING DISTRICTS AND OTHER GEOCHEMICAL ANOMALIES

1. Shingle Canyon district
2. Georgetown district
3. Fierro-Hanover district
4. Skate Canyon area
5. Central district
6. Sheep Corral Canyon area
7. Chloride Flat–Boston Hill districts
8. Fleming Camp area
9. Pinos Altos district
10. Juniper Hill area
11. Circle Mesa area

FIGURE 4.—Distribution of lead in the magnetic fraction. Contours drawn at 500, 1,000, 2,000, 5,000, 7,000, and 10,000 parts per million. In some places, contours are shifted as much as 1.1 km (one grid cell) from sample localities due to computer averaging technique.

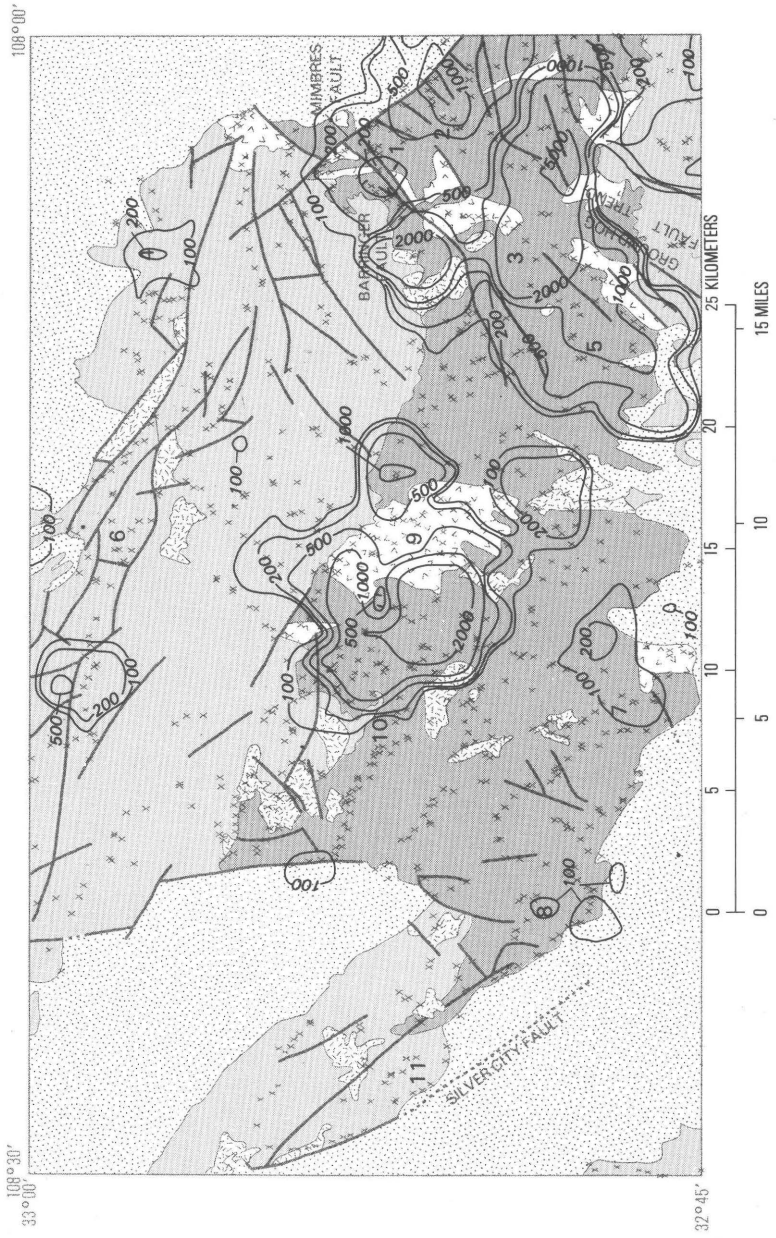
108°00'
108°30'
33°00'
32°45'
SILVER CITY FAULT
0
5
10
15
20
25 KILOMETERS
0
5
10
15 MILES

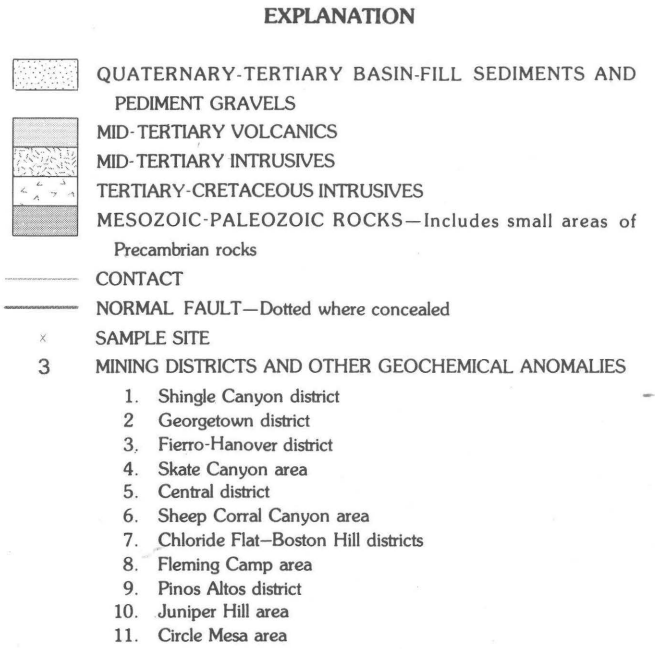

FIGURE 5.—Distribution of copper in the nonmagnetic fraction. Contours drawn at 100, 200, 500, 1,000, 2,000, and 5,000 parts per million; hachures indicate closed areas of lower values. In some places contours are shifted as much as 1.1 km (one grid cell) from sample localities due to computer averaging technique.

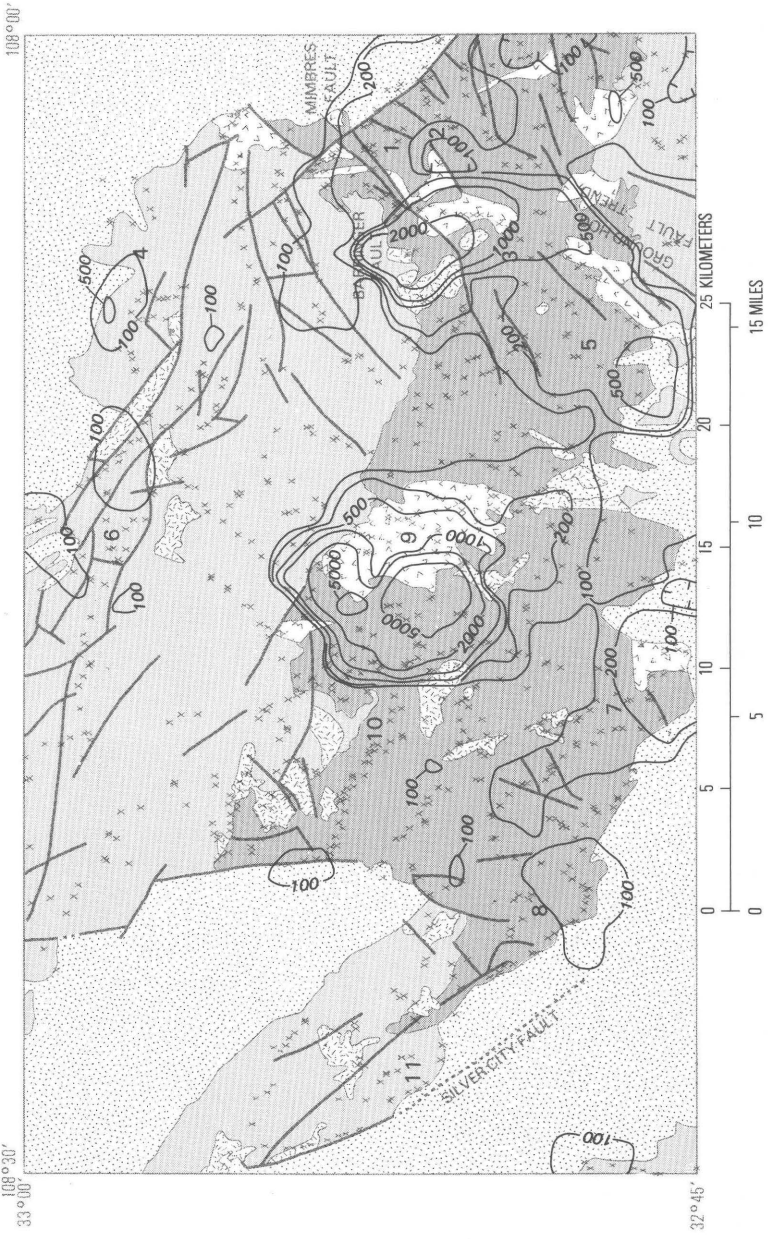
108°00'
108°30'
33°00'
32°45'
MIMBRES FAULT
BAYARD FAULT
GROUSE CANYON FAULT TREND
SILVER CITY FAULT
0
5
10
15
20
25 KILOMETERS
0
5
10
15 MILES

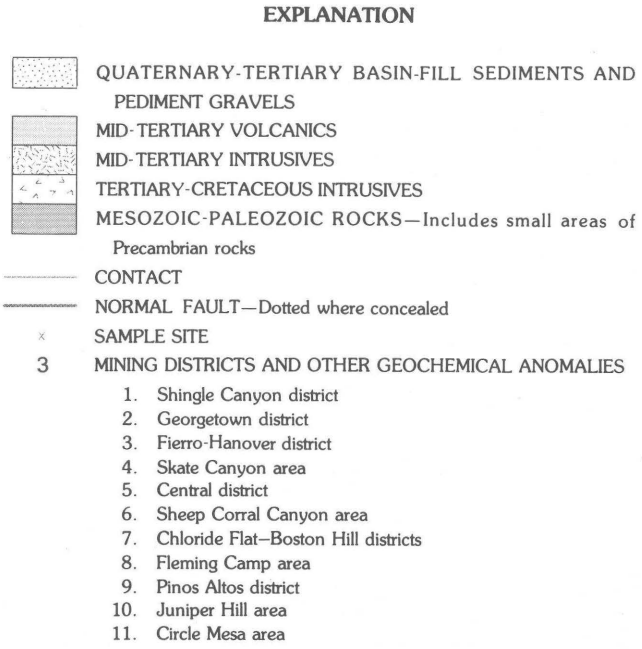

FIGURE 6.—Distribution of copper in the magnetic fraction. Contours drawn at 100, 200, 500, 1,000, 2,000, and 5,000 parts per million; hachures indicate closed areas of lower values. In some places, contours are shifted as much as 1.1 km (one grid cell) from sample localities due to computer averaging technique.

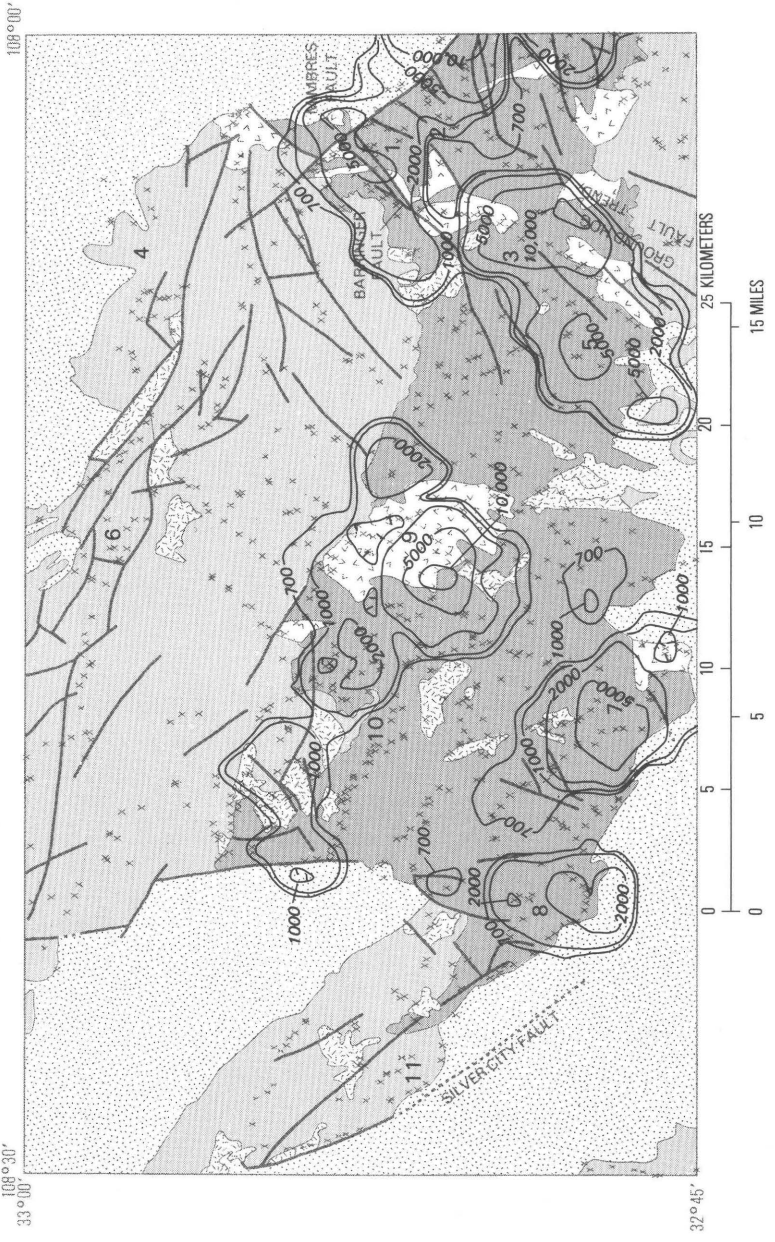
108°00'
108°30'
33°00'
32°45'
SILVER CITY FAULT
0
5
10
15
20
25 KILOMETERS
0
5
10
15 MILES

EXPLANATION

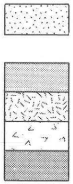

QUATERNARY-TERTIARY BASIN-FILL SEDIMENTS AND PEDIMENT GRAVELS

MID-TERTIARY VOLCANICS

MID-TERTIARY INTRUSIVES

TERTIARY-CRETACEOUS INTRUSIVES

MESOZOIC-PALEOZOIC ROCKS—Includes small areas of Precambrian rocks

CONTACT

NORMAL FAULT—Dotted where concealed

SAMPLE SITE

3 MINING DISTRICTS AND OTHER GEOCHEMICAL ANOMALIES

1. Shingle Canyon district
2. Georgetown district
3. Fierro-Hanover district
4. Skate Canyon area
5. Central district
6. Sheep Corral Canyon area
7. Chloride Flat–Boston Hill districts
8. Fleming Camp area
9. Pinos Altos district
10. Juniper Hill area
11. Circle Mesa area

FIGURE 7.—Distribution of zinc in the non-magnetic fraction. Contours drawn at 700, 1,000, 2,000, 5,000 and 10,000 parts per million; hachures indicate closed areas of lower values. In some places, contours are shifted as much as 1.1 km (one grid cell) from sample localities due to computer averaging technique.

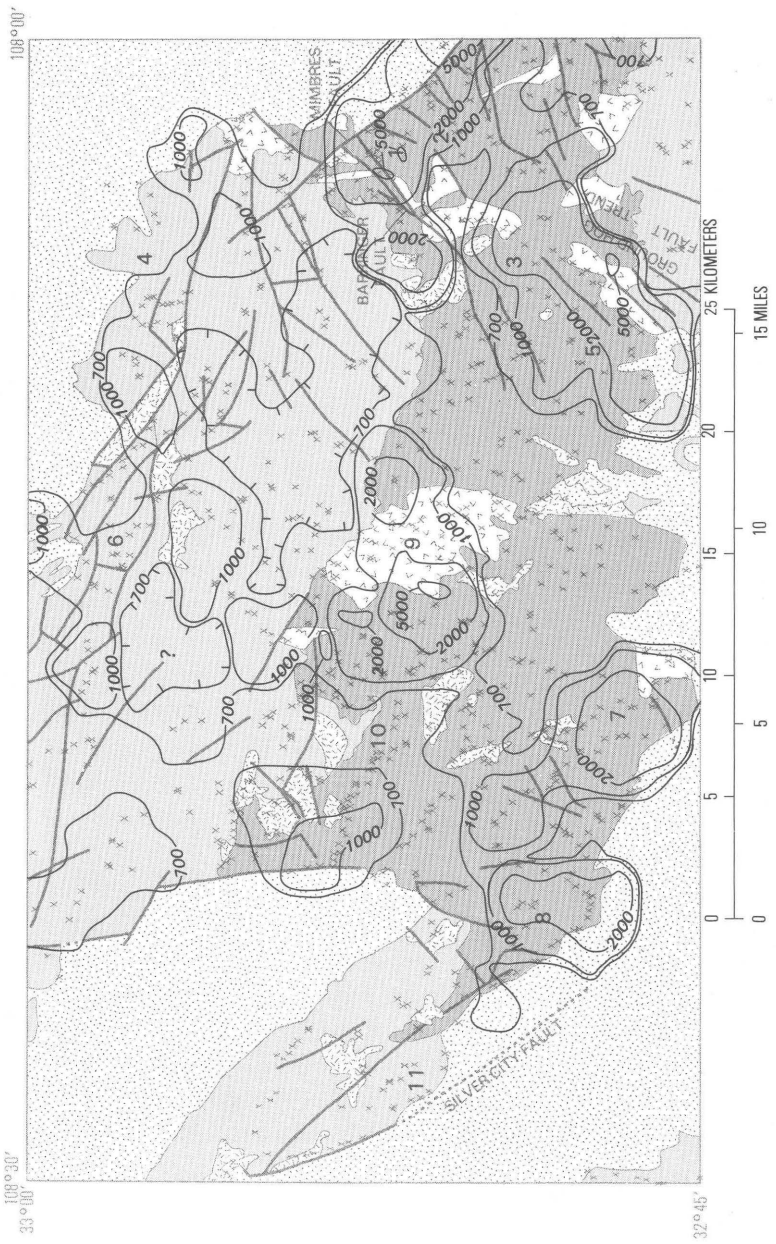
108°00'
108°30'
33°00'
32°45'
MIMBRES FAULT
BAYARD FAULT
GRO TRENDI FAULT
SILVER CITY FAULT
0 5 10 15 20 25 KILOMETERS
0 5 10 15 MILES

EXPLANATION

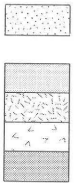

QUATERNARY-TERTIARY BASIN-FILL SEDIMENTS AND PEDIMENT GRAVELS

MID-TERTIARY VOLCANICS

MID-TERTIARY INTRUSIVES

TERTIARY-CRETACEOUS INTRUSIVES

MESOZOIC-PALEOZOIC ROCKS—Includes small areas of Precambrian rocks

CONTACT

NORMAL FAULT—Dotted where concealed

SAMPLE SITE

3 MINING DISTRICTS AND OTHER GEOCHEMICAL ANOMALIES

1. Shingle Canyon district
2. Georgetown district
3. Fierro-Hanover district
4. Skate Canyon area
5. Central district
6. Sheep Corral Canyon area
7. Chloride Flat–Boston Hill districts
8. Fleming Camp area
9. Pinos Altos district
10. Juniper Hill area
11. Circle Mesa area

FIGURE 8.—Distribution of zinc in the magnetic fraction. Contours drawn at 700, 1,000, 2,000 and 5,000 parts per million; hachures indicate closed areas of lower values; query within hachure indicates area of inadequate data. In some places, contours are shifted as much as 1.1 km (one grid cell) from sample localities due to computer averaging technique.

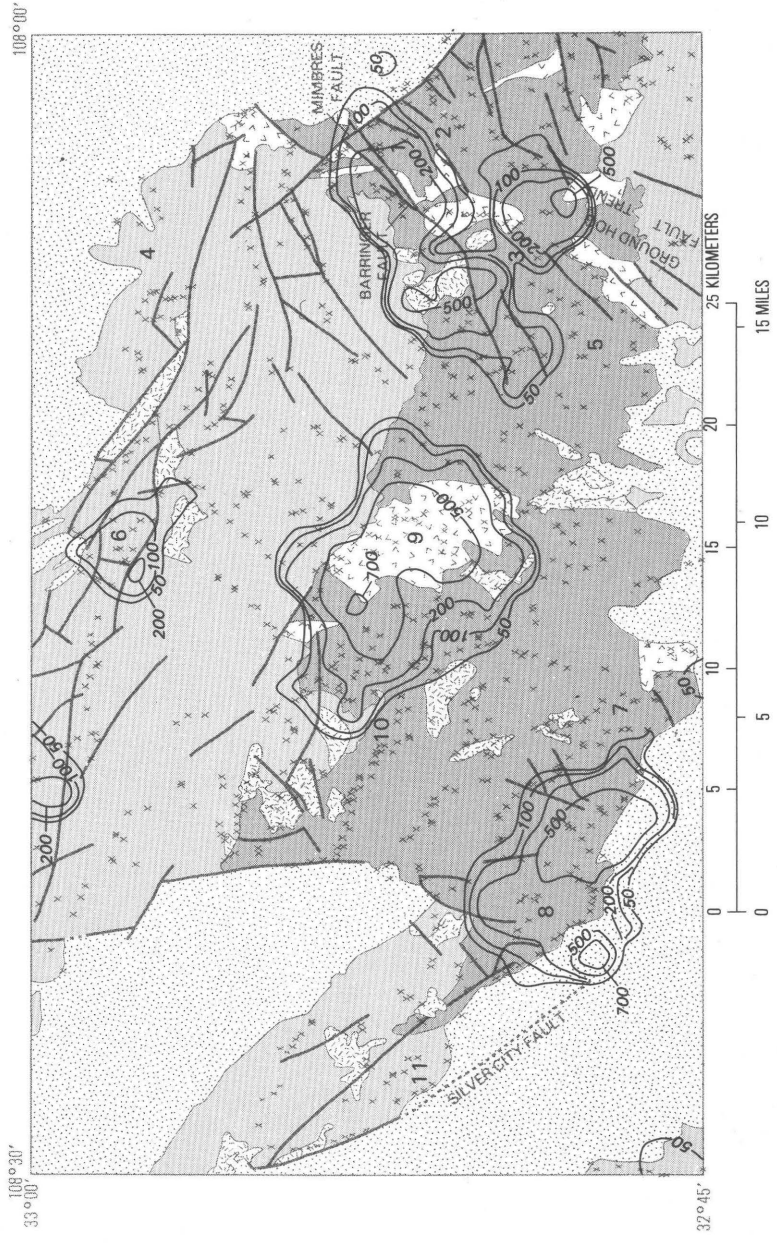
108°00'
108°30'
33°00'
32°45'
MIMBRES FAULT
BARRINGER FAULT
GROUND HOG TREND FAULT
SILVER CITY FAULT
1
2
3
4
5
6
7
8
9
10
11
50
100
200
500
700
0
5
10
15
20
25 KILOMETERS
0
5
10
15 MILES

EXPLANATION

QUATERNARY-TERTIARY BASIN-FILL SEDIMENTS AND PEDIMENT GRAVELS

MID-TERTIARY VOLCANICS

MID-TERTIARY INTRUSIVES

TERTIARY-CRETACEOUS INTRUSIVES

MESOZOIC-PALEOZOIC ROCKS—Includes small areas of Precambrian rocks

CONTACT

NORMAL FAULT—Dotted where concealed

SAMPLE SITE

3 MINING DISTRICTS AND OTHER GEOCHEMICAL ANOMALIES

1. Shingle Canyon district
2. Georgetown district
3. Fierro-Hanover district
4. Skate Canyon area
5. Central district
6. Sheep Corral Canyon area
7. Chloride Flat–Boston Hill districts
8. Fleming Camp area
9. Pinos Altos district
10. Juniper Hill area
11. Circle Mesa area

FIGURE 9.—Distribution of bismuth in the nonmagnetic fraction. Contours drawn at 50, 100, 200, 500, and 700 parts per million. In some places, contours are shifted as much as 1.1 km (one grid cell) from sample localities due to computer averaging technique.

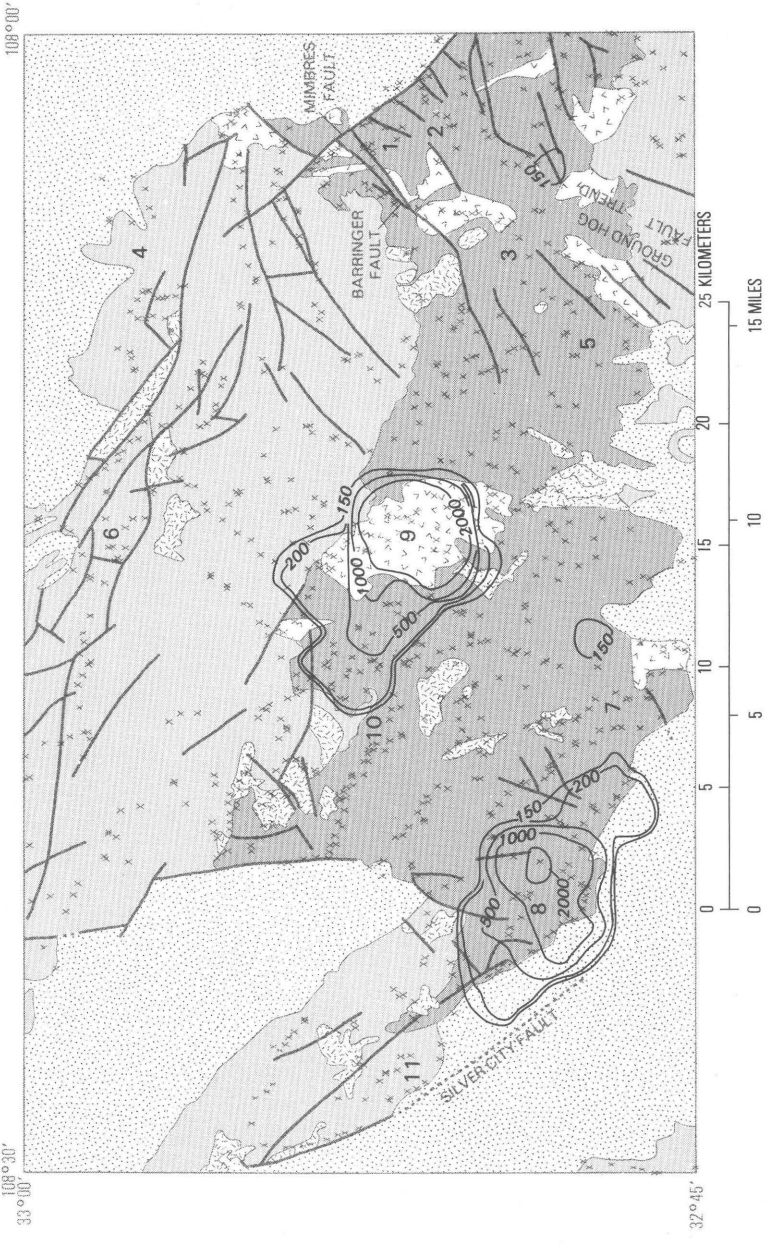
108°00'
108°30'
33°00'
32°45'
MIMBRES FAULT
BARRINGER FAULT
GROUND HOG TREND
FAULT
SILVER CITY FAULT
1
2
3
4
5
6
7
8
9
10
11
150
200
500
1000
2000
0
5
10
15
20
25 KILOMETERS
0
5
10
15 MILES

EXPLANATION

QUATERNARY-TERTIARY BASIN-FILL SEDIMENTS AND PEDIMENT GRAVELS

MID-TERTIARY VOLCANICS

MID-TERTIARY INTRUSIVES

TERTIARY-CRETACEOUS INTRUSIVES

MESOZOIC-PALEOZOIC ROCKS—Includes small areas of Precambrian rocks

CONTACT

NORMAL FAULT—Dotted where concealed

SAMPLE SITE

3 MINING DISTRICTS AND OTHER GEOCHEMICAL ANOMALIES

1. Shingle Canyon district
2. Georgetown district
3. Fierro-Hanover district
4. Skate Canyon area
5. Central district
6. Sheep Corral Canyon area
7. Chloride Flat–Boston Hill districts
8. Fleming Camp area
9. Pinos Altos district
10. Juniper Hill area
11. Circle Mesa area

FIGURE 10.—Distribution of tungsten in the nonmagnetic fraction. Contours drawn at 150, 200, 500, 1,000 and 2,000 parts per million. In some places, contours are shifted as much as 1.1 km (one grid cell) from sample localities due to computer averaging technique.

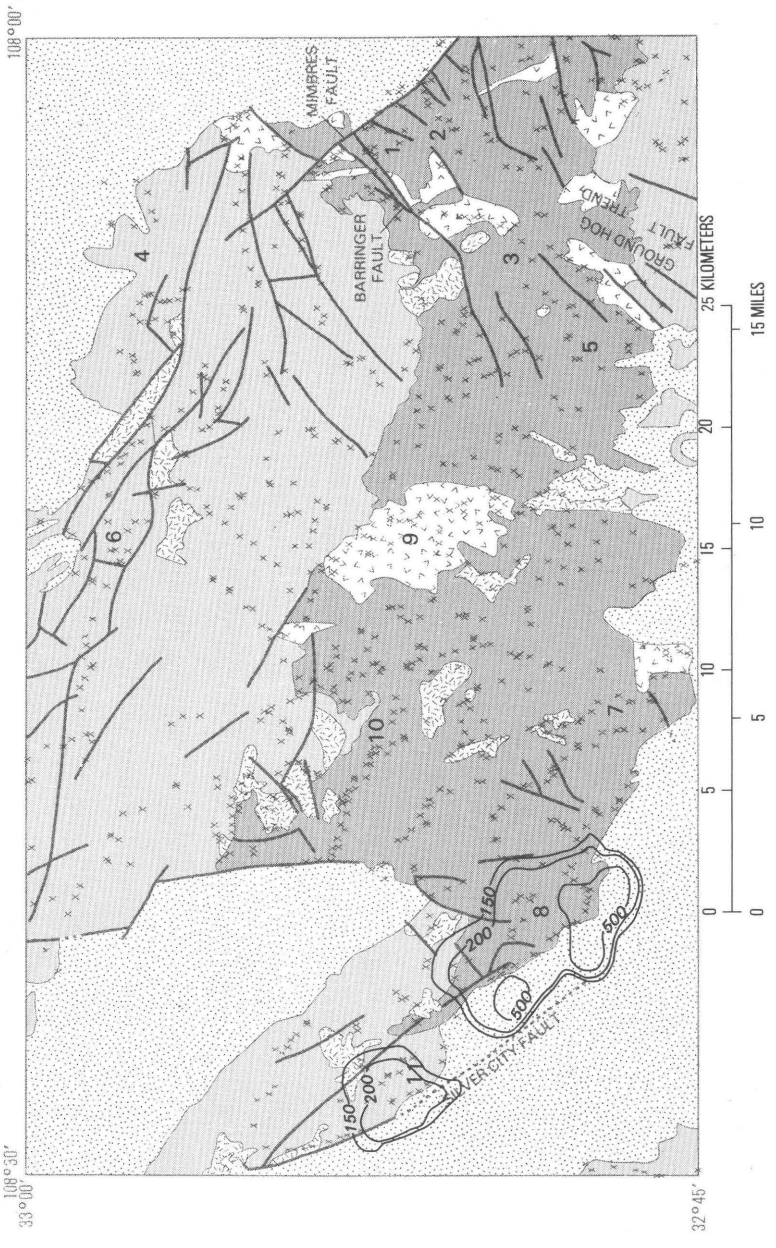
108°00'
108°30'
33°00'
32°45'
MIMBRES FAULT
BARRINGER FAULT
GROUND HOG TREND FAULT
SILVER CITY FAULT
1
2
3
4
5
6
7
8
9
10
150
200
500
0
5
10
15
20
25 KILOMETERS
0
5
10
15 MILES

EXPLANATION

QUATERNARY-TERTIARY BASIN-FILL SEDIMENTS AND PEDIMENT GRAVELS

MID-TERTIARY VOLCANICS

MID-TERTIARY INTRUSIVES

TERTIARY-CRETACEOUS INTRUSIVES

MESOZOIC-PALEOZOIC ROCKS—Includes small areas of Precambrian rocks

CONTACT

NORMAL FAULT—Dotted where concealed

SAMPLE SITE

3 MINING DISTRICTS AND OTHER GEOCHEMICAL ANOMALIES

1. Shingle Canyon district
2. Georgetown district
3. Fierro-Hanover district
4. Skate Canyon area
5. Central district
6. Sheep Corral Canyon area
7. Chloride Flat–Boston Hill districts
8. Fleming Camp area
9. Pinos Altos district
10. Juniper Hill area
11. Circle Mesa area

FIGURE 11.—Distribution of tungsten in the magnetic fraction. Contours drawn at 150, 200, and 500 parts per million. In some places, contours are shifted as much as 1.1 km (one grid cell) from sample localities due to computer averaging technique.

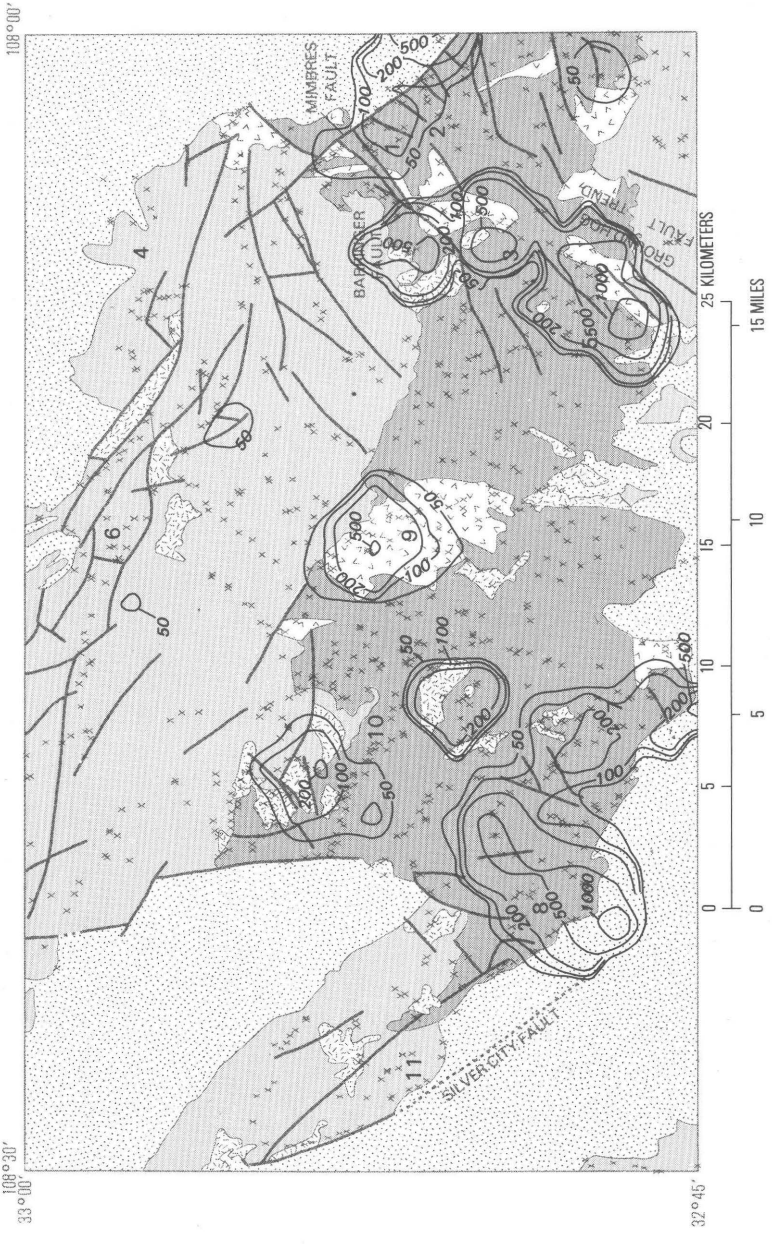
108°00'
108°30'
33°00'
32°45'
MIMBRES FAULT
BARRINGER HILL FAULT
GROUNDHOG TRENDS FAULT
SILVER CITY FAULT
4
6
9
10
11
8
2
3
50
100
200
500
1000
0
5
10
15
20
25 KILOMETERS
0
5
10
15 MILES

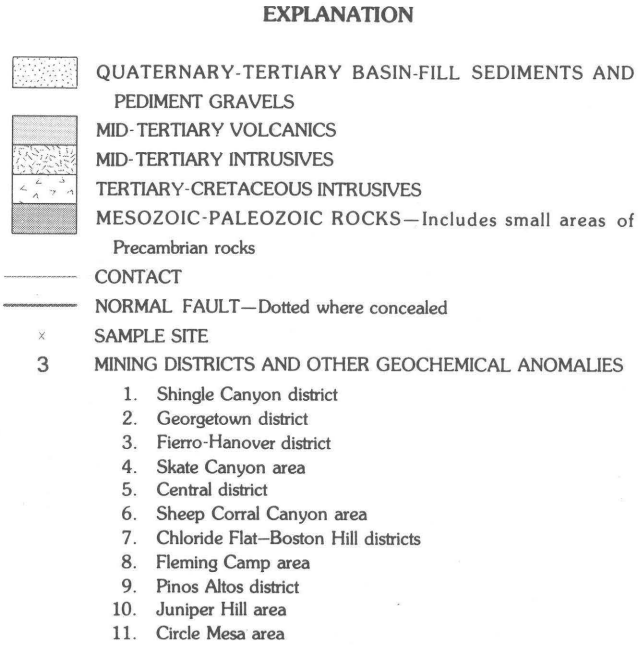

FIGURE 12.—Distribution of molybdenum in the non-magnetic fraction. Contours drawn at 50, 100, 200, 500, and 700 parts per million. In some places, contours are shifted as much as 1.1 km (one grid cell) from sample localities due to computer averaging technique.

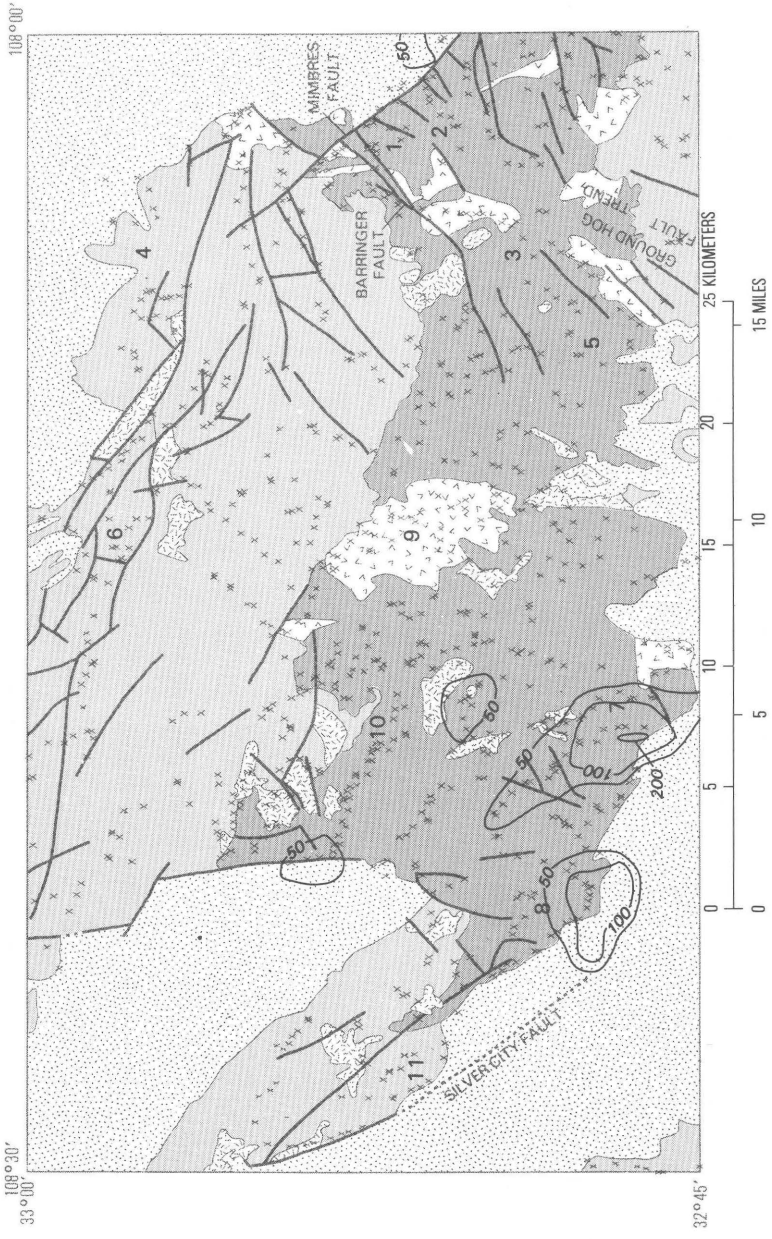
108°00'
33°00'
108°30'
32°45'
MIMBRES FAULT
BARRINGER FAULT
GROUND HOG TREND FAULT
SILVER CITY FAULT
1
2
3
4
5
6
8
9
10
11
50
100
200
0
5
10
15
20
25 KILOMETERS
0
5
10
15 MILES

EXPLANATION

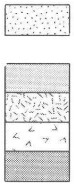

QUATERNARY-TERTIARY BASIN-FILL SEDIMENTS AND PEDIMENT GRAVELS

MID-TERTIARY VOLCANICS

MID-TERTIARY INTRUSIVES

TERTIARY-CRETACEOUS INTRUSIVES

MESOZOIC-PALEOZOIC ROCKS—Includes small areas of Precambrian rocks

CONTACT

NORMAL FAULT—Dotted where concealed

SAMPLE SITE

3 MINING DISTRICTS AND OTHER GEOCHEMICAL ANOMALIES

1. Shingle Canyon district
2. Georgetown district
3. Fierro-Hanover district
4. Skate Canyon area
5. Central district
6. Sheep Corral Canyon area
7. Chloride Flat–Boston Hill districts
8. Fleming Camp area
9. Pinos Altos district
10. Juniper Hill area
11. Circle Mesa area

FIGURE 13.—Distribution of molybdenum in the magnetic fraction. Contours drawn at 50 and 100 parts per million. In some places, contours are shifted as much as 1.1 km (one grid cell) from sample localities due to computer averaging technique.

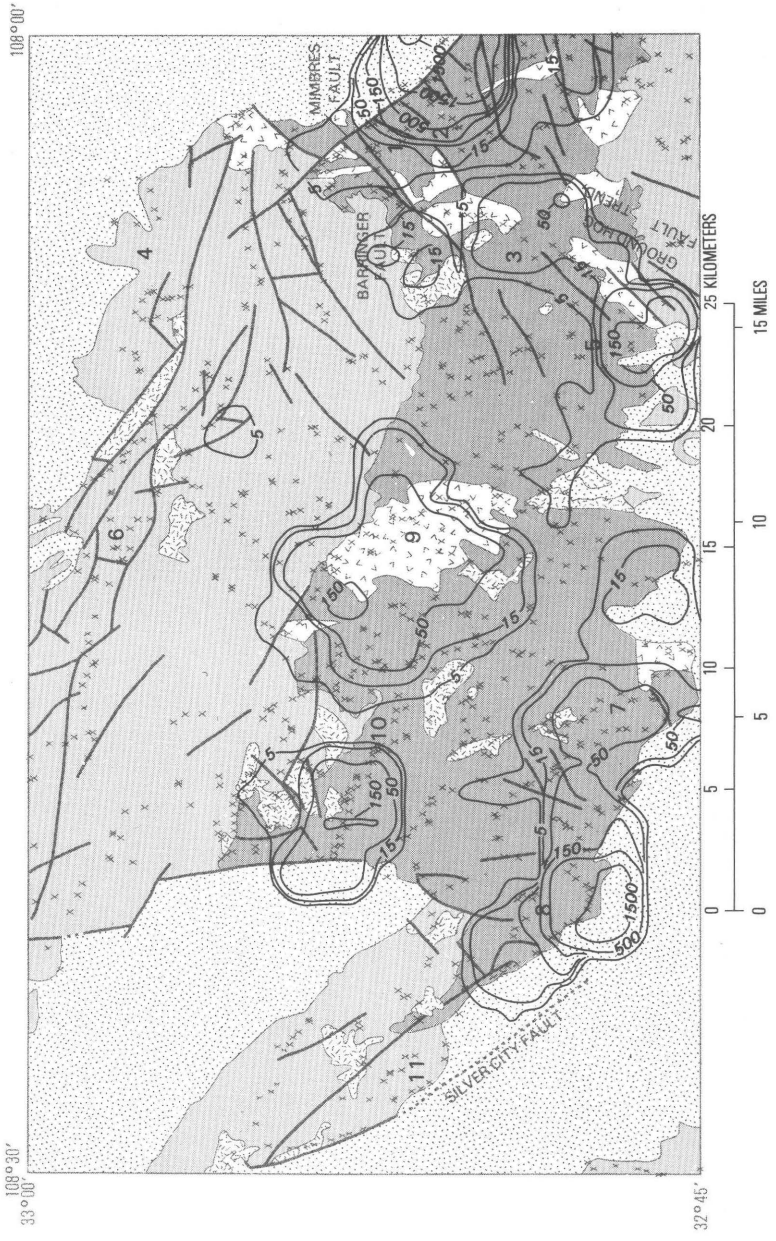
108°00'
33°00'
108°30'
32°45'
MIMBRES FAULT
BARRINGER FAULT
GROUND HOG TREND FAULT
SILVER CITY FAULT
1
2
3
4
5
6
7
8
9
10
11
15
50
150
500
1500
0
5
10
15
25 KILOMETERS
0
5
10
15 MILES

EXPLANATION

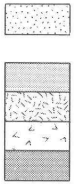

QUATERNARY-TERTIARY BASIN-FILL SEDIMENTS AND PEDIMENT GRAVELS

MID-TERTIARY VOLCANICS

MID-TERTIARY INTRUSIVES

TERTIARY-CRETACEOUS INTRUSIVES

MESOZOIC-PALEOZOIC ROCKS—Includes small areas of Precambrian rocks

CONTACT

NORMAL FAULT—Dotted where concealed

SAMPLE SITE

3 MINING DISTRICTS AND OTHER GEOCHEMICAL ANOMALIES

1. Shingle Canyon district
2. Georgetown district
3. Fierro-Hanover district
4. Skate Canyon area
5. Central district
6. Sheep Corral Canyon area
7. Chloride Flat–Boston Hill districts
8. Fleming Camp area
9. Pinos Altos district
10. Juniper Hill area
11. Circle Mesa area

FIGURE 14.—Distribution of silver in the nonmagnetic fraction. Contours drawn at 5, 15, 50, 150, 500, and 1,500 parts per million. In some places, contours are shifted as much as 1.1 km (one grid cell) from sample localities due to computer averaging technique.

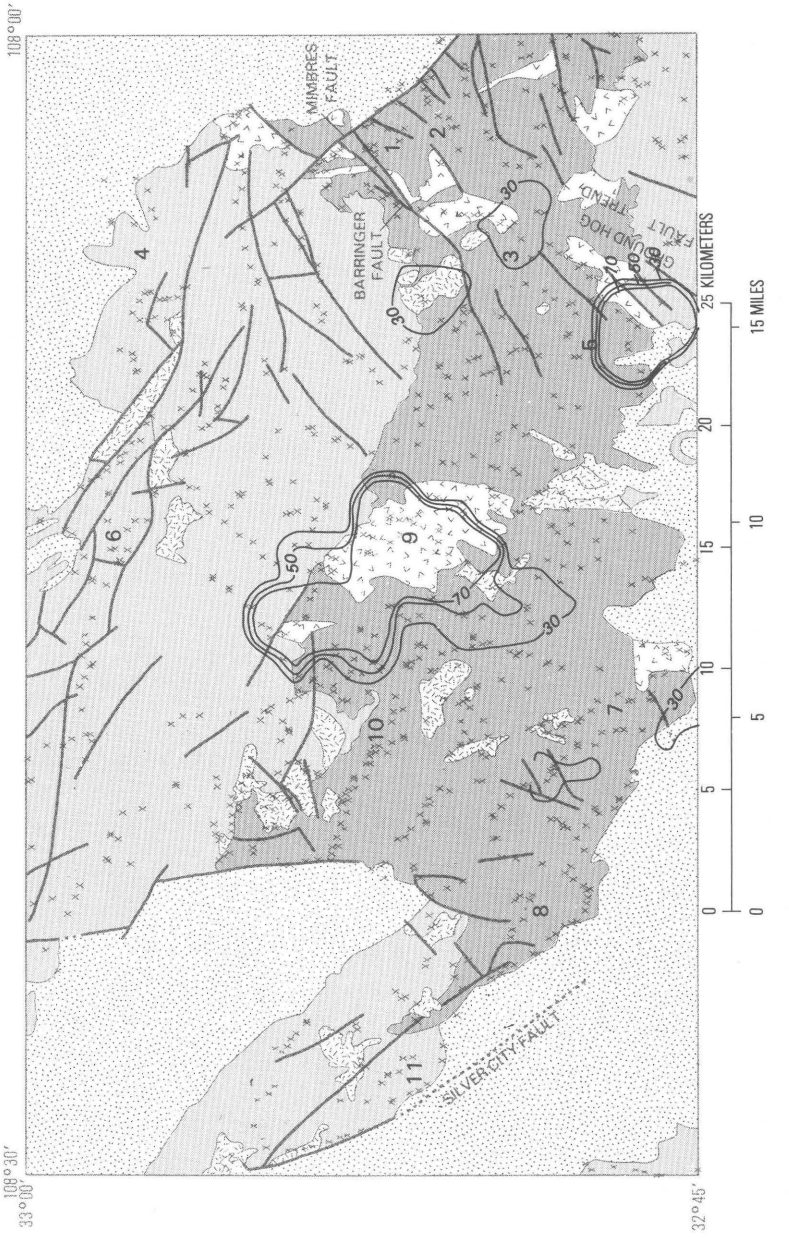
108°00'
108°30'
33°00'
32°45'
MIMBRES FAULT
BARRINGER FAULT
GUND HOG TREND
FAULT
SILVER CITY FAULT
1
2
3
4
5
6
7
8
9
10
11
30
50
70
90
0
5
10
15
20
25 KILOMETERS
0
5
10
15 MILES

EXPLANATION

QUATERNARY-TERTIARY BASIN-FILL SEDIMENTS AND PEDIMENT GRAVELS

MID-TERTIARY VOLCANICS

MID-TERTIARY INTRUSIVES

TERTIARY-CRETACEOUS INTRUSIVES

MESOZOIC-PALEOZOIC ROCKS—Includes small areas of Precambrian rocks

CONTACT

NORMAL FAULT—Dotted where concealed

× SAMPLE SITE

3 MINING DISTRICTS AND OTHER GEOCHEMICAL ANOMALIES

1. Shingle Canyon district
2. Georgetown district
3. Fierro-Hanover district
4. Skate Canyon area
5. Central district
6. Sheep Corral Canyon area
7. Chloride Flat–Boston Hill districts
8. Fleming Camp area
9. Pinos Altos district
10. Juniper Hill area
11. Circle Mesa area

FIGURE 15.—Distribution of silver in the magnetic fraction. Contours drawn at 5, 15, and 50 parts per million. In some places, contours are shifted as much as 1.1 km (one grid cell) from sample localities due to computer averaging technique.

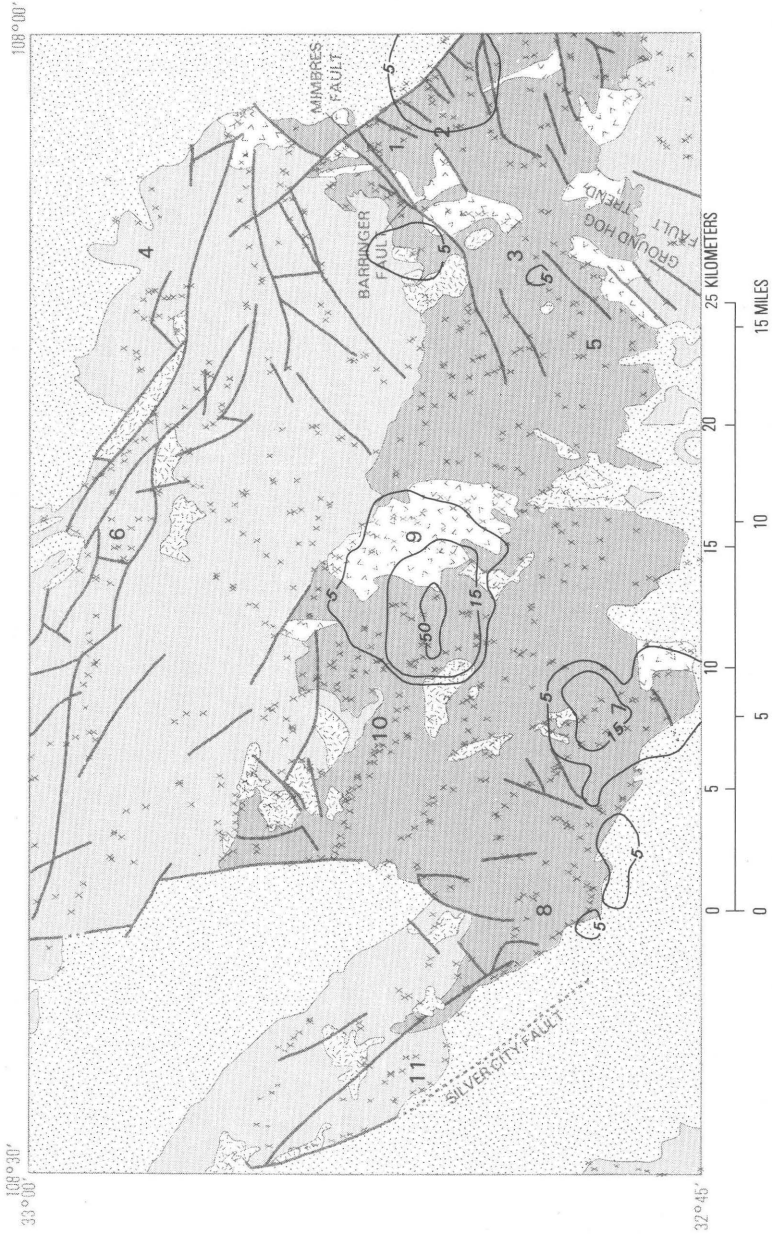
108°00'
33°00'
108°30'
32°45'
MIMBRES FAULT
BARRINGER FAULT
GROUND HOG FAULT TREND
SILVER CITY FAULT
1
2
3
4
5
6
8
9
10
11
5
15
50
0
5
10
15
20
25 KILOMETERS
0
5
10
15 MILES

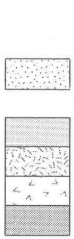

EXPLANATION

QUATERNARY-TERTIARY BASIN-FILL SEDIMENTS AND PEDIMENT GRAVELS

MID-TERTIARY VOLCANICS

MID-TERTIARY INTRUSIVES

TERTIARY-CRETACEOUS INTRUSIVES

MESOZOIC-PALEOZOIC ROCKS—Includes small areas of Precambrian rocks

CONTACT

NORMAL FAULT—Dotted where concealed

× SAMPLE SITE

3 MINING DISTRICTS AND OTHER GEOCHEMICAL ANOMALIES

1. Shingle Canyon district
2. Georgetown district
3. Fierro-Hanover district
4. Skate Canyon area
5. Central district
6. Sheep Corral Canyon area
7. Chloride Flat–Boston Hill districts
8. Fleming Camp area
9. Pinos Altos district
10. Juniper Hill area
11. Circle Mesa area

FIGURE 16.—Distribution of gold in the nonmagnetic fraction. Contours drawn at 30, 50, and 70 parts per million. In some places, contours are shifted as much as 1.1 km (one grid cell) from sample localities due to computer averaging technique.

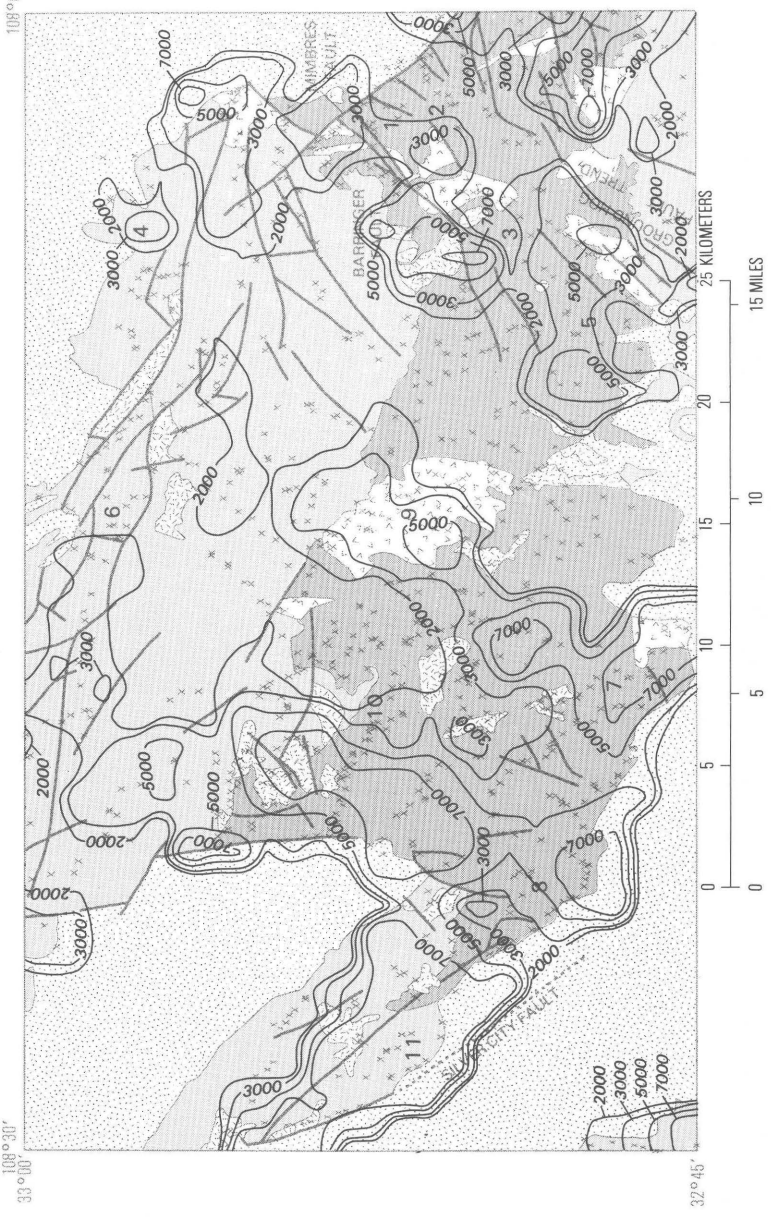
108°00'
33°00'
108°30'
32°45'
HIMBRES FAULT
BARRINGER HILL FAULT
GROUNDWATER TREND
SILVER CITY FAULT
0
5
10
15
20
25 KILOMETERS
0
5
10
15 MILES

EXPLANATION

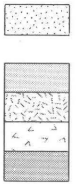

QUATERNARY-TERTIARY BASIN-FILL SEDIMENTS AND PEDIMENT GRAVELS

MID-TERTIARY VOLCANICS

MID-TERTIARY INTRUSIVES

TERTIARY-CRETACEOUS INTRUSIVES

MESOZOIC-PALEOZOIC ROCKS—Includes small areas of Precambrian rocks

CONTACT

NORMAL FAULT—Dotted where concealed

SAMPLE SITE

3 MINING DISTRICTS AND OTHER GEOCHEMICAL ANOMALIES

1. Shingle Canyon district
2. Georgetown district
3. Fierro-Hanover district
4. Skate Canyon area
5. Central district
6. Sheep Corral Canyon area
7. Chloride Flat–Boston Hill districts
8. Fleming Camp area
9. Pinos Altos district
10. Juniper Hill area
11. Circle Mesa area

FIGURE 17.—Distribution of barium in the nonmagnetic fraction. Contours drawn at 2,000, 3,000, 5,000 and 7,000 parts per million. In some places, contours are shifted as much as 1.1 km (one grid cell) from sample localities due to computer averaging technique.

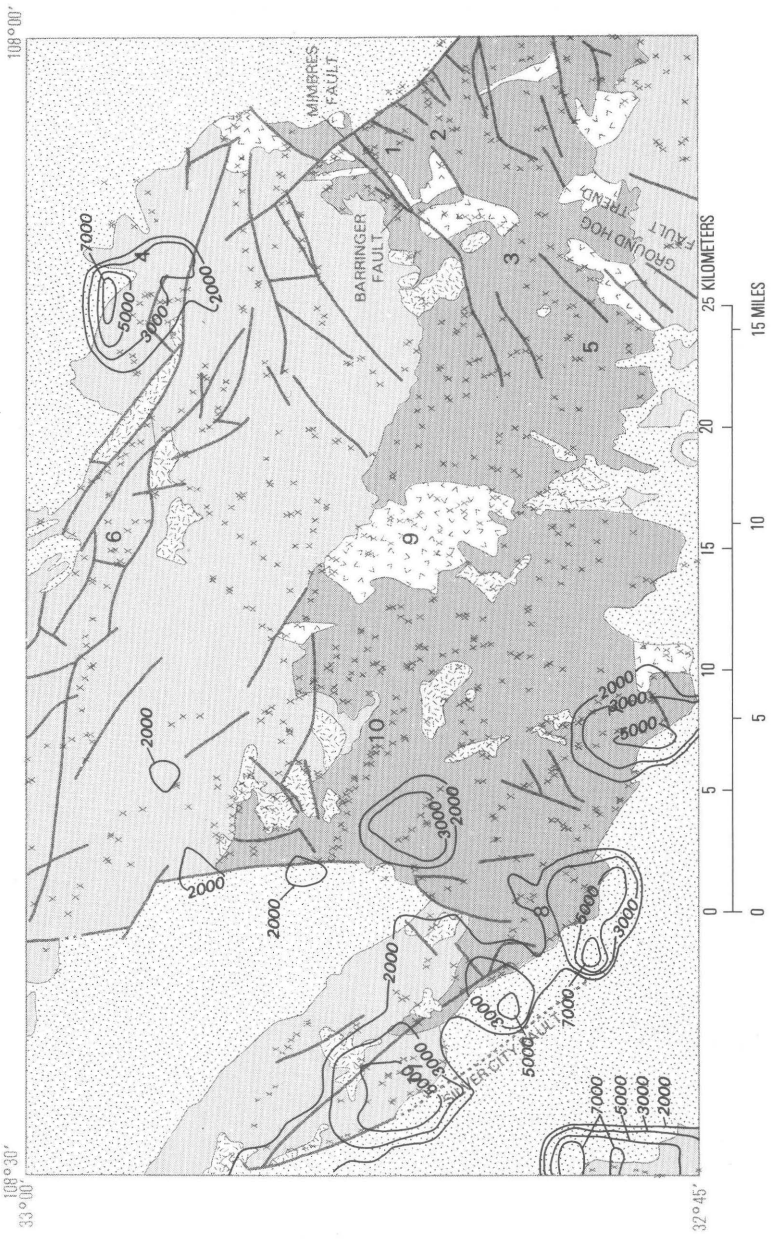
108°00'
33°00'
108°30'
32°45'
MIMBRES FAULT
BARRINGER FAULT
GROUND HOG TREND FAULT
SILVER CITY FAULT
1
2
3
4
5
6
7
8
9
10
11
7000
5000
3000
2000
0
5
10
15
20
25 KILOMETERS
0
5
10
15 MILES

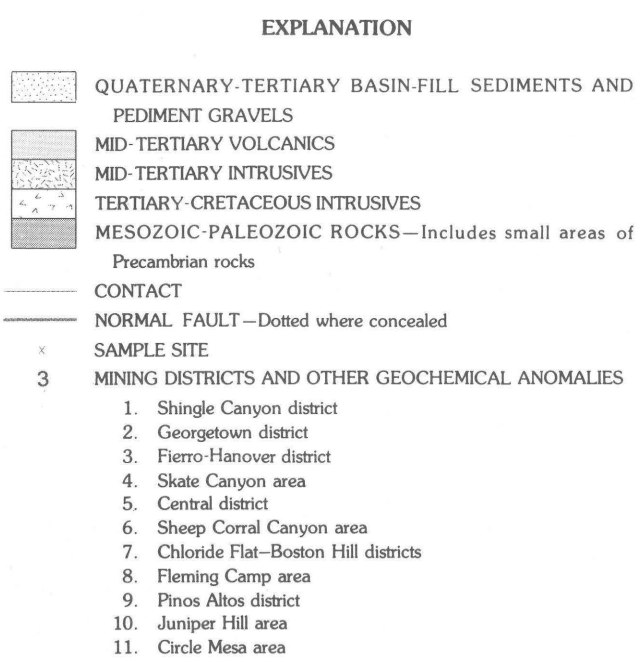

FIGURE 18.—Distribution of barium in the magnetic fraction. Contours drawn at 2,000, 3,000, and 5,000 parts per million. In some places, contours are shifted as much as 1.1 km (one grid cell) from sample localities due to computer averaging technique.

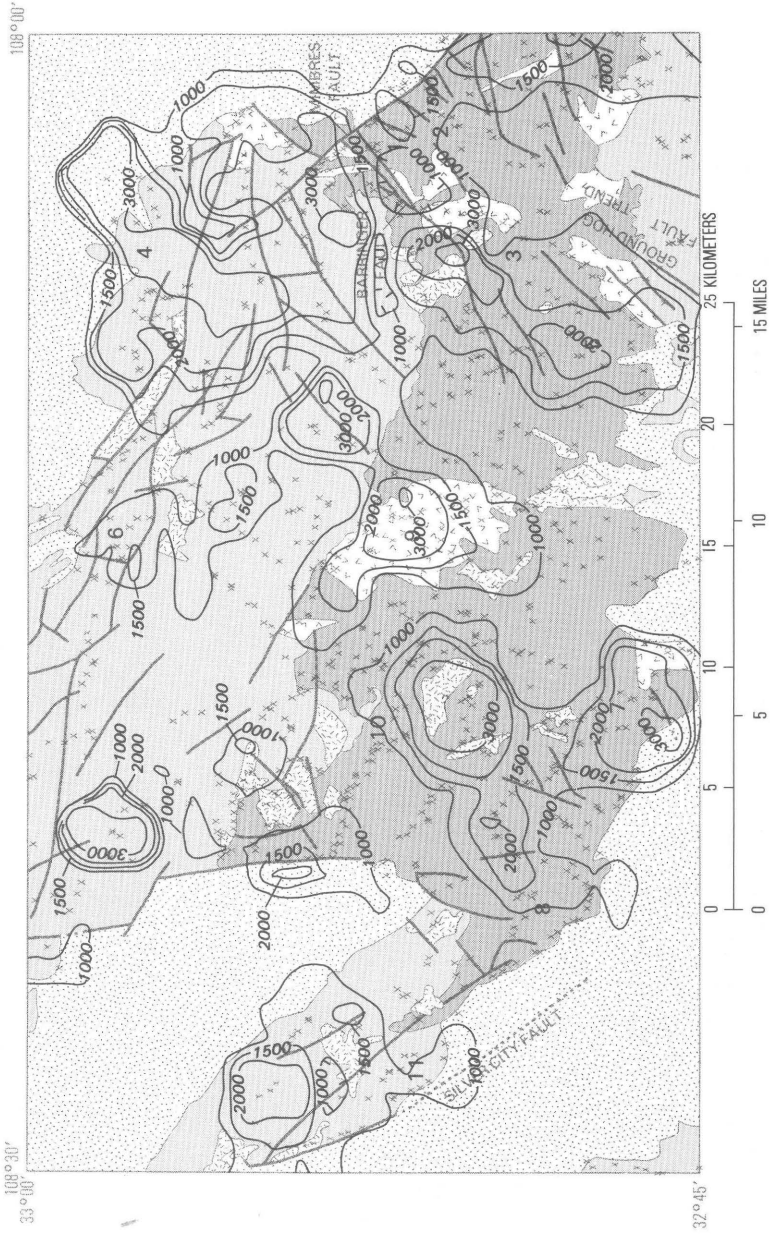
108°00'
108°30'
33°00'
32°45'
HANOVER-FIERRO FAULT
BARRINGER HILL FAULT
GROUNDHOG TREND
SILVER CITY FAULT
1
2
3
4
6
8
10
0
5
10
15
20
25 KILOMETERS
0
10
15 MILES

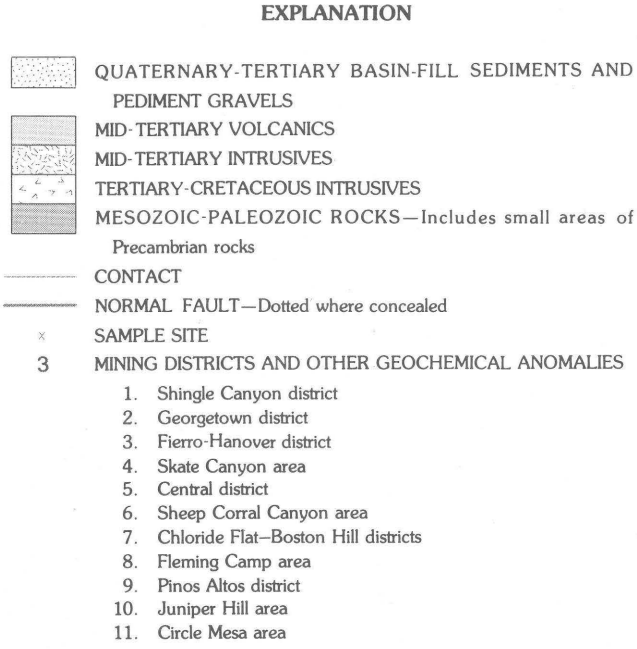

FIGURE 19.—Distribution of manganese in the nonmagnetic fraction. Contours drawn at 1,000, 1,500, 2,000, and 3,000 parts per million; hachures indicate closed areas of lower values. In some places, contours are shifted as much as 1.1 km (one grid cell) from sample localities due to computer averaging technique.

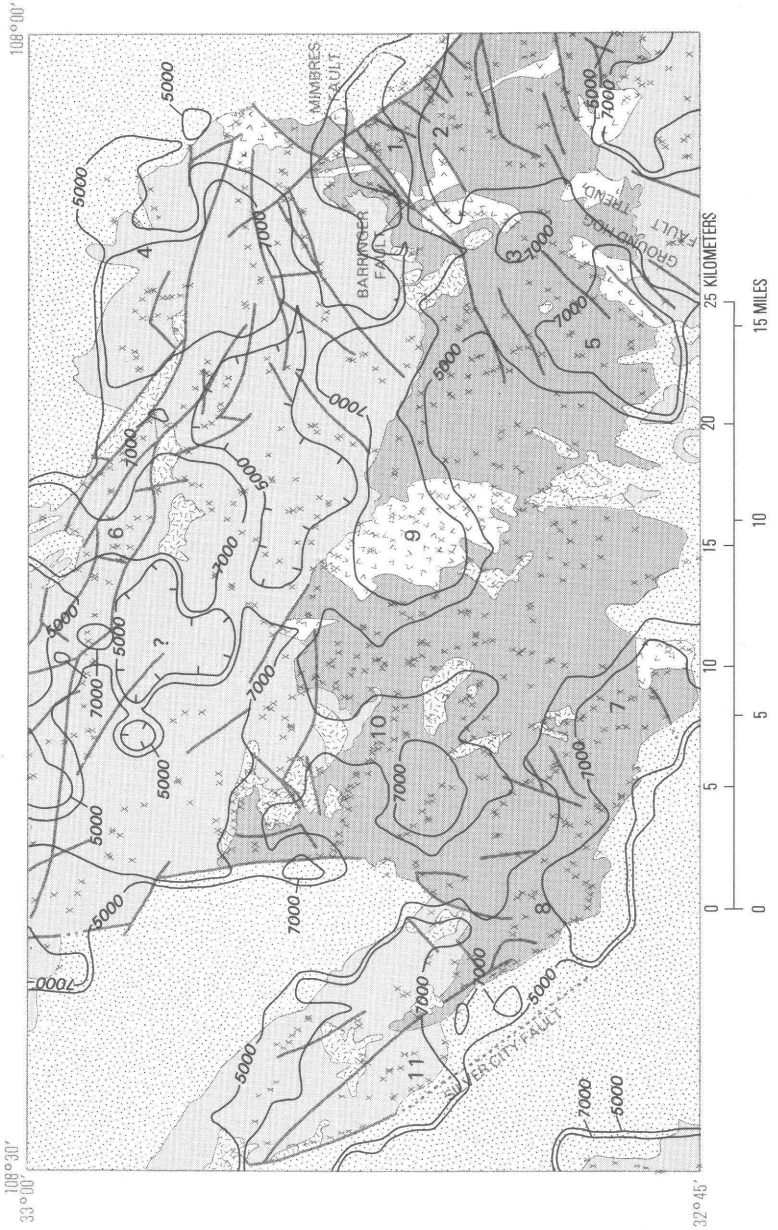
108°00'
33°00'
108°30'
32°45'
MIMBRES FAULT
BARRINGER FAULT
GROUNDHOG TRENDS FAULT
SILVER CITY FAULT
5000
7000
1000
1
2
3
4
5
6
7
8
9
10
11
?
0
5
10
15
20
25 KILOMETERS
0
5
10
15 MILES

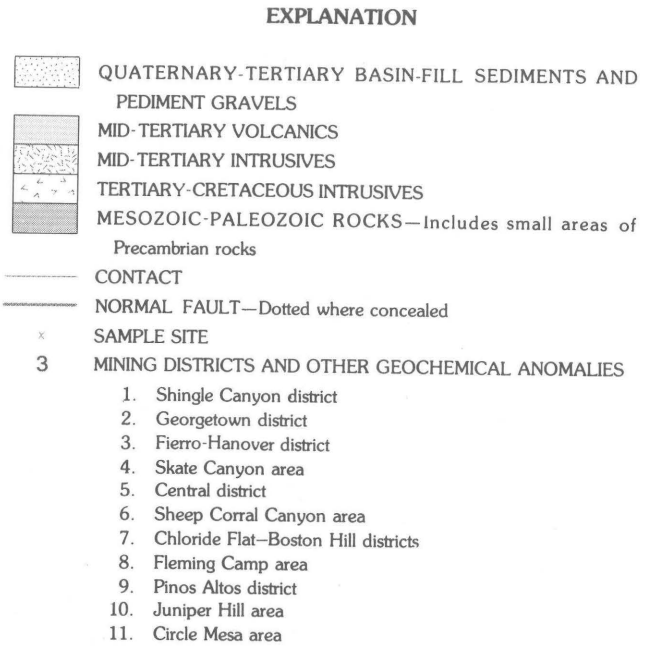

FIGURE 20.—Distribution of manganese in the magnetic fraction. Contours drawn at 5,000 and 7,000 parts per million; hachures indicate areas of lower values; query within hachure indicates area of inadequate data. In some places, contours are shifted as much as 1.1 km (one grid cell) from sample localities due to computer averaging technique.

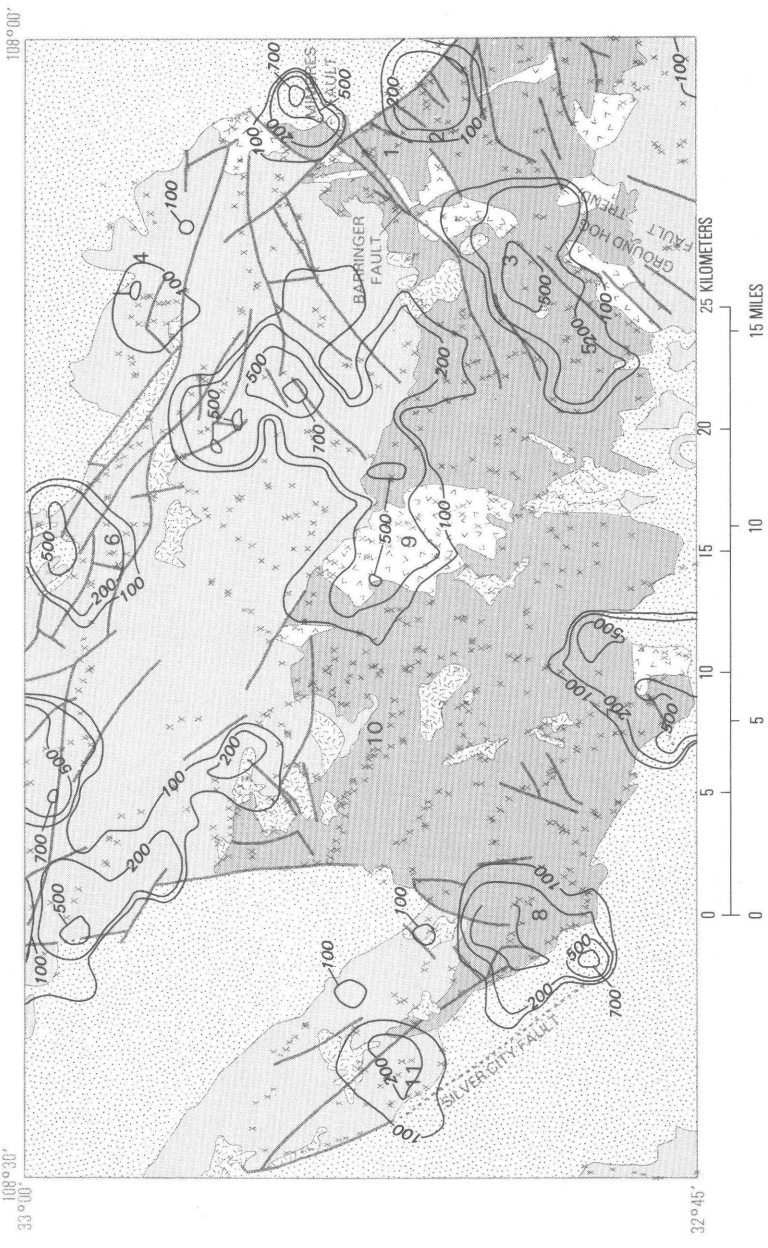
108°00'
108°30'
33°00'
32°45'
BARRINGER FAULT
SILVER CITY FAULT
0
5
10
15
20
25 KILOMETERS
0
5
10
15 MILES

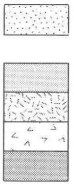

EXPLANATION

QUATERNARY-TERTIARY BASIN-FILL SEDIMENTS AND PEDIMENT GRAVELS

MID-TERTIARY VOLCANICS

MID-TERTIARY INTRUSIVES

TERTIARY-CRETACEOUS INTRUSIVES

MESOZOIC-PALEOZOIC ROCKS—Includes small areas of Precambrian rocks

CONTACT

NORMAL FAULT—Dotted where concealed

SAMPLE SITE

3 MINING DISTRICTS AND OTHER GEOCHEMICAL ANOMALIES

1. Shingle Canyon district
2. Georgetown district
3. Fierro-Hanover district
4. Skate Canyon area
5. Central district
6. Sheep Corral Canyon area
7. Chloride Flat–Boston Hill districts
8. Fleming Camp area
9. Pinos Altos district
10. Juniper Hill area
11. Circle Mesa area

FIGURE 21.—Distribution of tin in the nonmagnetic fraction. Contours drawn at 100, 200, 500, and 1,000 parts per million. In some places, contours are shifted as much as 1.1 km (one grid cell) from sample localities due to computer averaging technique.

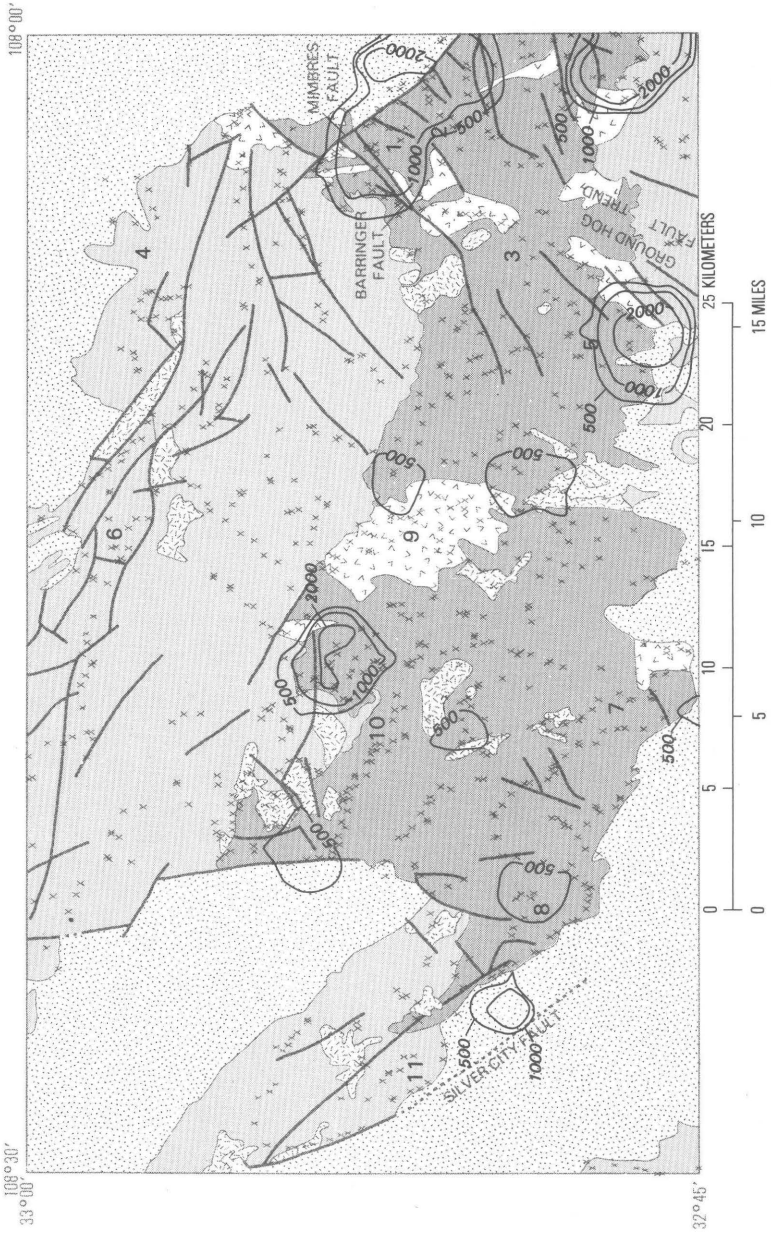
108°00'
108°30'
33°00'
32°45'
MIMBRES FAULT
BARRINGER FAULT
GROUND HOG TRENDS FAULT
SILVER CITY FAULT
1
2
3
4
5
6
7
8
9
10
11
2000
1000
500
0
5
10
15
20
25 KILOMETERS
0
5
10
15 MILES

EXPLANATION

QUATERNARY-TERTIARY BASIN-FILL SEDIMENTS AND PEDIMENT GRAVELS

MID-TERTIARY VOLCANICS

MID-TERTIARY INTRUSIVES

TERTIARY-CRETACEOUS INTRUSIVES

MESOZOIC-PALEOZOIC ROCKS—Includes small areas of Precambrian rocks

CONTACT

NORMAL FAULT—Dotted where concealed

SAMPLE SITE

3 MINING DISTRICTS AND OTHER GEOCHEMICAL ANOMALIES

1. Shingle Canyon district
2. Georgetown district
3. Fierro-Hanover district
4. Skate Canyon area
5. Central district
6. Sheep Corral Canyon area
7. Chloride Flat–Boston Hill districts
8. Fleming Camp area
9. Pinos Altos district
10. Juniper Hill area
11. Circle Mesa area

FIGURE 22.—Distribution of vanadium in the nonmagnetic fraction. Contours drawn at 500, 1,000, and 2,000 parts per million. In some places contours are shifted as much as 1.1 km (one grid cell) from sample localities due to computer averaging technique.

TABLE 1.—*Location and description of window areas*

Window area	Geographic boundaries deg min s	deg min s	Geologic environment	Deposit type	References
Shingle Canyon district--------	32 52 00 108 03 00	32 54 00 108 04 30	Ore localized in Pennsylvanian limestone beneath Perman and Pennsylvanian shales. Localized at intersection of Barringer and Mimbres faults.	Replacement Zn-Pb----------	Kelly, 1958, p. 33-36; Jones and others, 1967.
Georgetown district----------	32 49 00 108 00 00	32 52 00 108 03 00	Ore localized in Silurian Fusselman Dolomite beneath Devonian Percha Shale. Near intersection Mimbres fault and northeast dike and fault trend extending outward from Santa Rita (Chino).	Fissure veins and replacement Ag-Pb lodes. Restricted to oxide zone.	Lasky and Wooten, 1933, p. 56-57; Hernon, 1953, p. 138-140; Jones and others, 1961, 1967; Jones and Hernon, 1973.
Fierro-Hanover district --------	32 49 00 108 04 00	32 51 00 108 07 30	Ore localized chiefly within contact metamorphic zone (skarn) surrounding Laramide quartz diorite-granodiorite stock.	Contact metamorphic Fe-Zn and skarn replacement Zn-Cu-Pb.	Lasky and Wooten, 1933, p. 52-53; Schmitt, 1939; Hernon and others, 1953; Jones and Hernon, 1973.
Skate Canyon----------	32 56 00 108 06 00	32 58 00 108 09 30	Tertiary volcanics----------	None known----------	Moore, 1953.
Central district----------	32 45 00 108 05 00	32 49 00 108 11 00	Ore localized by faults dikes and fissures in Paleozoic carbonate rocks and shales. Trend of faults mainly northeast referred to as Groundhog Trend.	Vein deposits of Zn-Cu-Pb-Ag and minor Au placers.	Lasky and Wooten, 1933, p. 51-52; Lasky, 1936; Jones and others, 1961, 1967; Jones and Hernon, 1973.
Sheep Corral Canyon----------	32 56 30 108 10 00	33 00 00 108 16 00	Tertiary volcanics cut by northwest-trending block faults, intruded by rhyolite dikes and irregular bodies.	None known----------	Finnell, 1976a.
Chloride Flat and Boston Hill districts.	32 45 00 108 15 00	32 48 00 108 18 00	Ore localized by faults and fissures in Paleozoic shales and carbonate rocks. Ag veins localized in Silurian Fusselman Dolomite beneath Devonian Percha shale.	Weathered and leached Mn-Fe deposits at Boston Hill. Ag halide vein and replacement bodies at Chloride Flat. Restricted to oxide zone.	Lasky and Wooten, 1933, p. 52, 65-66; Entwhistle, 1944; Hernon, 1953; Cunningham, 1974.
Fleming Camp----------	32 46 00 108 19 00	32 51 00 108 25 00	Ore localized as pods in Cretaceous Beartooth Quartzite.	Ag halide replacement deposits. Restricted to oxide zone.	Lasky and Wooten, 1933, p. 56; Hernon, 1953, p. 138.
Pinos Altos district----------	32 47 30 108 10 00	32 54 00 108 17 30	Ore localized within Laramide quartz monzonite stock and within skarns developed in Paleozoic carbonates and shales and Cretaceous sandstones, shales, and andesite.	Vein deposits Au-Ag-Cu-Pb-Zn within stock. Skarn-replacement Zn-Cu-Pb-Ag in surrounding host rocks and gold placers.	Paige, 1916; Lasky and Wooten, 1933, p. 58-59; Hernon, 1953, p. 140; McKnight and Fellows, 1978.
Juniper Hill district----------	32 52 00 108 17 30	32 56 00 108 22 30	Prospects on faults and fractures---	None known----------	None available.
Circle Mesa ----------	32 50 00 108 26 30	32 53 00 108 29 00	Tertiary tuffs and flows intruded by felsic plugs and dikes.	None known----------	Trauger, 1972.

TABLE 2.—*Ratio of fraction magnitudes for selected metals within the window areas*

[FM ratio = $\frac{\text{Anomaly intensity X area (M-lamp fraction)}}{\text{Anomaly intensity X area (NM-lamp fraction)}}$ where Intensity = $\frac{\text{Anomaly mean}}{\text{Threshold}}$; for the chalcophilic elements Aq, Bi, Cu, Mo, Pb, and Zn, this ratio may indicate, particularly in the mining districts, the degree to which sulfides and other ore minerals are weathered, sometimes redistributed and then fixed in the seconday oxides of iron and manganese within the supergene zone. High ratios indicate a large factor for secondary processes; low ratio indicates a large factor for epigenetic ore-minerals and their secondary ore-mineral products; for lithophile elements Mn, Ba, Be, Sn, and W, ratio is high where element is predominately associated with various oxides of manganese and iron or magnetic primary minerals and low where discrete nonmagnetic primary minerals of that metal are present in abundance. Threshold values are as in table 3. NM, indicates anomalous in nonmagnetic fraction only and therefore may be equated with a value of 0; M, anomalous in magnetic fraction only and therefore may be equated to an infinitely large number. ---, no anomaly; >, greater than value shown]

Window area	Element											Ratio sum[1]
	Mn	Aq	Ba	Be	Bi	Cu	Mo	Pb	Sn	W	Zn	
Skate Canyon	4.03	---	27.00	NM	---	1.09	---	NM	NM	---	35.80	36.89
Circle Mesa	8.50	---	1.98	1.33	---	5.34	NM	NM	M	29.51	5.50	10.84
Chloride Flat-Boston Hill district	2.26	0.25	1.20	3.78	0.32	2.50	0.48	0.35	M	M	2.54	6.44
Fleming Camp area	13.57	0.005	0.67	0.47	0.01	1.83	0.19	0.77	0.38	0.32	1.58	4.38
Pinos Altos district	6.26	0.23	0.21	NM	0.18	1.77	0.05	0.11	0.03	0.01	1.22	3.56
Shingle Canyon district	2.86	NM	NM	NM	0.50	0.59	0.04	0.10	NM	---	2.22	3.45
Fierro-Hanover district	8.00	NM	NM	---	NM	1.80	0.01	0.04	NM	0.75	1.15	3.00
Sheep Corral Canyon	24.19	---	0.14	NM	NM	2.75	NM	NM	NM	---	M	>2.75
Juniper Hill district	13.49	0.02	0.67	4.22	NM	0.97	0.22	0.22	NM	1.95	1.19	2.62
Georgetown district	14.14	0.01	NM	M	NM	0.31	0.17	0.39	0.40	---	1.62	2.50
Central district	5.91	0.03	0.12	0.10	0.28	0.31	0.02	0.16	NM	NM	0.77	1.57
Ratio sum[2]	103.21	0.54	31.99	>9.90	1.29	19.26	1.18	2.14	>0.81	>32.54	>53.59	256.54

[1]Chalcophilic elements only; single area.

[2]Single element; all areas.

TABLE 3.—*Comparison of magnitudes for selected metals*

Element	Concentrate fraction	Threshold value	Number of samples	Number of anomalous samples	Sum of anomalous values	Mean anomalous value	Intensity (mean/ threshold)	Area (percent anomalous)	Magnitude (EM) (Intensity X Area)	REM (cumulative percent magnitude)
				Georgetown district						
Ag-------	NM	5.0	35	21	24,015	1,144	228.71	60.00	13,722	79
Cu-------	NM	100	35	26	25,100	965	9.65	74.29	717	4.1
Pb-------	NM	500	35	15	95,000	6,333	12.67	42.86	543	3.1
Zn-------	M	500	35	31	85,600	2,761	5.52	88.57	489	2.8
Zn-------	NM	500	35	13	52,800	4,062	8.12	37.14	302	1.7
Co-------	M	30	35	32	2,700	84	2.81	91.43	257	1.5
Mo-------	NM	50	35	7	4,020	574	11.49	20.00	230	1.3
Cu-------	M	100	35	26	7,700	296	2.96	74.29	220	1.3
V--------	NM	500	35	18	37,000	2,056	4.11	51.43	211	1.2
Pb-------	M	500	35	14	36,700	2,621	5.24	40.00	210	1.2
Mn-------	M	2,000	35	21	99,000	4,714	2.36	60.00	141	0.8
Ag-------	M	5.0	35	9	242	27	5.38	25.71	138	0.8
N--------	M	500	35	20	12,100	605	1.21	57.14	69	0.4
Mo-------	M	50	35	9	690	76	1.53	25.71	39	0.2
Sn-------	NM	100	35	7	1,250	179	1.79	20.00	36	0.2
Ba-------	NM	2,000	35	4	20,000	5,000	2.50	11.43	29	0.2
Bi-------	NM	50	35	3	350	117	2.33	8.57	20	0.1
Sn-------	M	100	35	1	500	500	5.00	2.86	14	0.1
Co-------	NM	30	35	4	140	35	1.17	11.43	13	0.1
Mg-------	M	1.5	35	4	6.5	1.6	1.08	11.43	12	0.1
Mg-------	NM	1.5	35	3	6.5	2.2	1.44	8.57	12	0.1
Mn-------	MN	2,000	35	2	7,000	3500	1.75	5.71	10	0.1
Be-------	NM	15	35	1	15	15	1,000.0	2.86	3	0.0
							Total Magnitude (EM)----------		17,438	

Fleming Camp area

Ag-------	NM	5	83	18	19,292	1,072	214.36	21.69	4649	52
Pb-------	NM	500	83	38	277,200	7,295	14.59	45.78	668	7.4
W--------	NM	100	83	30	43,700	1,457	14.57	36.14	527	5.9
Pb-------	M	500	83	39	213,700	5,479	10.96	46.99	515	5.7
Mo-------	NM	50	83	25	15,990	640	12.79	30.12	385	4.3
Bi-------	NM	50	83	24	11,820	492	9.85	28.92	285	3.2
Co-------	M	30	83	79	6,830	86	2.88	95.18	274	3.1
Mn-------	M	2,000	83	66	380,000	5,758	2.88	79.52	229	2.6
Zn-------	M	500	83	52	77,000	1,481	2.96	62.65	186	2.1
W--------	M	100	83	29	14,200	490	4.90	34.94	171	1.9
Mg-------	MN	1.5	83	40	198	4.96	3.31	48.19	159	1.8
Mg-------	M	1.5	83	43	163	3.79	2.53	51.81	131	1.5
Zn-------	NM	500	83	26	48,600	1,869	3.74	31.33	117	1.3
V--------	M	500	83	48	35,500	740	1.48	57.83	86	1.0
Ba-------	NM	2,000	83	24	132,000	5,500	2.75	28.92	80	0.9
Mo-------	M	50	83	29	2,980	103	2.06	34.94	72	0.8
Cu-------	M	100	83	35	5,400	154	1.54	42.17	65	0.7
Be-------	NM	15	83	22	770	35	2.33	21.51	62	0.7
Sn-------	NM	100	83	15	5,000	333	3.33	18.07	60	0.7
Ba-------	M	2,000	83	21	88,000	4,190	2.10	25.30	53	0.6
V--------	NM	500	83	13	15,900	1,223	2.45	15.66	38	0.4
Cu-------	NM	100	83	15	2,950	197	1.97	18.07	36	0.4
Be-------	M	15	83	17	365	21	1.43	20.48	29	0.3
Ag-------	M	5	83	6	104	17	3.47	7.23	25	0.3
Au-------	NM	20	83	7	390	56	2.79	8.43	23	0.3
Sn-------	M	100	83	4	1,900	475	4.75	4.82	23	0.3
Mn-------	NM	2,000	83	11	28,110	2,545	1.27	13.25	17	0.2
Bi-------	M	50	83	1	150	150	3.00	1.20	3.6	0.0
Co-------	NM	30	73	3	90	30	1.00	3.61	3.6	0.0

Total Magnitude (EM)---------- 8,972

TABLE 3.—*Comparison of magnitudes for selected metals—Continued*

Element	Concentrate fraction	Threshold value	Number of samples	Number of anomalous samples	Sum of anomalous values	Mean anomalous value	Intensity (mean/ threshold)	Area (percent anomalous)	Magnitude (EM) (Intensity X Area)	REM (cumulative percent magnitude)
				Central district						
Pb--------	NM	500	46	29	364,500	12,569	25.14	63.04	1585	24
Cu--------	NM	100	46	32	46,550	1,455	14.55	69.57	1012	16
Mo--------	NM	50	46	14	14,550	1,039	20.79	30.43	633	9.7
Ag--------	NM	5	46	15	1,377	92	18.36	32.61	599	9.2
Zn--------	NM	500	46	25	125,200	5,008	10.02	54.35	544	8.3
Zn--------	M	500	46	39	96,910	2,485	4.97	84.78	421	6.4
Cu--------	M	100	46	33	14,350	435	4.35	71.74	312	4.8
Co--------	M	30	46	45	4,160	92	3.08	97.83	301	4.6
Pb--------	M	500	46	22	60,100	2,732	5.46	47.83	261	4.0
Mn--------	M	2,000	46	34	195,000	5,735	2.87	73.91	212	3.2
Sn--------	NM	100	46	8	5,750	719	7.19	17.39	125	1.9
Mg--------	M	15	46	15	62	4	2.78	32.61	91	1.4
V---------	NM	500	46	12	20,200	1,683	3.37	26.09	88	1.3
Co--------	NM	30	46	14	1,150	82	2.74	30.43	83	1.3
Ba--------	NM	2,000	46	13	68,000	5,231	2.62	28.26	74	1.1
V---------	M	500	46	21	12,400	590	1.18	45.65	54	0.8
Mn--------	NM	2,000	46	12	33,000	2,750	1.38	26.09	36	0.5
Be--------	NM	15	46	7	145	21	1.38	15.22	21	0.3
Ag--------	M	5	46	3	42	14	2.80	6.52	13	0.3
Ba--------	NM	50	46	3	350	117	2.33	6.52	15	0.2
Mo--------	M	50	46	3	270	90	1.80	6.52	12	0.2
Mg--------	NM	1.5	46	4	6	1.5	1.00	8.70	8.7	0.1
Ba--------	M	2,000	46	4	8,000	2,000	1.00	8.70	8.7	0.1
Au--------	M	20	46	1	70	70	3.50	2.17	7.6	0.1
Au--------	NM	20	46	2	40	20	1.00	4.35	4.4	0.1
Bi--------	M	50	46	1	100	100	2.00	2.17	4.4	0.1
W---------	NM	100	46	1	150	150	1.50	2.17	3.3	0.0
Be--------	M	15	46	1	15	15	1.00	2.17	2.2	0.0
							Total Magnitude (EM)----------		6,536	

Pinos Altos district

Cu--------	M	100	182	103	233,550	2,267	22.67	56.59	1,283	21
Pb--------	NM	500	182	73	781,300	10,703	21.41	40.11	859	14
Cu--------	NM	100	182	63	131,900	2,094	20.94	34.62	725	12
Ag--------	NM	5	182	53	6,290	119	23.74	29.12	691	11
Mg--------	M	1.5	182	179	1,123	6.3	4.88	98.35	411	6.8
W---------	NM	100	182	25	68,250	2,730	27.30	13.74	375	6.2
Co--------	M	30	182	173	15,290	88	2.95	95.05	280	4.6
Bi--------	NM	50	182	40	21,740	543	10.87	21.98	239	3.9
Mn--------	M	2,000	182	158	676,000	4,278	2.14	86.81	186	3.1
Ag--------	M	5	182	24	1,428	59	11.90	13.19	157	2.6
Zn--------	NM	500	182	50	124,100	2,482	4.96	27.47	136	2.2
Zn--------	M	500	182	37	101,900	2,754	5.51	20.33	112	1.8
V---------	M	500	182	139	91,900	661	1.32	76.37	101	1.7
Pb--------	M	500	182	30	86,700	2,890	5.78	16.48	95	1.6
Mo--------	NM	50	179	27	7,690	285	5.70	15.08	86	1.4
V---------	NM	500	182	26	60,100	2,312	4.62	14.29	66	1.1
Sn--------	NM	100	182	20	10,600	531	5.30	10.99	58	1.0
Au--------	NM	20	182	12	1,760	147	7.33	6.59	48	0.8
Bi--------	M	50	182	14	3,860	276	5.51	7.69	42	0.7
Co--------	NM	30	182	26	2,110	81	2.71	14.29	39	0.6
Mn--------	NM	2,000	182	30	108,000	3,600	1.80	16.48	30	0.5
Ba--------	NM	2,000	182	32	108,000	3,375	1.69	17.58	30	0.5
Mg--------	NM	1.5	182	18	41	2.3	1.52	9.89	15	0.2
Ba--------	M	2,000	182	7	23,000	3,286	1.64	3.85	6.3	0.1
Mo--------	M	50	182	7	420	60	1.20	3.85	4.6	0.1
W---------	M	100	182	5	600	120	1.20	2.75	3.3	0.1
Be--------	NM	15	182	4	65	16	1.08	2.20	2.4	0.0
Sn--------	M	100	182	3	350	117	1.17	1.65	1.9	0.0

Total Magnitude (EM)---------- 6,083

TABLE 3.—*Comparison of magnitudes for selected metals—Continued*

Element	Concentrate fraction	Threshold value	Number of samples	Number of anomalous samples	Sum of anomalous values	Mean anomalous value	Intensity (mean/ threshold)	Area (percent anomalous)	Magnitude (EM) (Intensity X Area)	REM (cumulative percent magnitude)
				Chloride Flat-Boston Hill district						
Pb-------	NM	500	17	15	109,700	7,313	14.63	88.24	1291	22
Ag-------	NM	5	17	9	992	110	22.04	52.94	1167	20
Pb-------	M	500	18	14	41,000	2,929	5.86	77.78	456	7.9
Zn-------	M	500	18	15	39,600	2,640	5.28	83.33	440	7.7
Sn-------	NM	100	17	6	6,350	1,058	10.58	35.29	374	6.5
Co-------	M	30	18	17	1,960	115	3.84	94.44	363	6.3
Ag-------	M	5	18	8	264	33	6.60	44.44	293	5.1
Cu-------	NM	100	18	14	4,500	321	3.21	77.78	250	4.4
Zn-------	NM	500	17	7	14,700	2,100	4.20	41.18	173	3.0
Mo-------	NM	50	17	6	1,090	182	3.63	35.29	128	2.2
Mn-------	M	2,000	18	8	43,000	5,375	2.69	44.44	119	2.1
Cu-------	NM	100	17	5	1,700	340	3.40	29.41	100	1.7
Ba-------	M	2,000	18	10	2,800	2,800	1.40	55.56	78	1.4
Mg-------	NM	1.5	17	5	19	3.8	2.53	29.41	75	1.3
V--------	M	500	18	9	5,900	656	1.31	50.00	66	1.1
Ba-------	NM	2,000	17	5	22,000	4,400	2.20	29.41	65	1.1
Mg-------	M	1.5	18	8	16	2.1	1.38	44.44	61	1.1
Mo-------	M	50	18	8	550	68.8	1.38	44.44	61	1.1
Mn-------	NM	2,000	17	5	18,000	3,600	1.80	29.41	53	0.9
Au-------	NM	20	17	2	100	50	2.50	11.76	29	0.5
W--------	NM	100	17	2	400	200	2.00	11.76	24	0.4
Be-------	M	15	18	4	60	15	1.00	22.22	22	0.4
Bi-------	NM	50	17	1	150	150	3.00	5.88	18	0.3
V--------	NM	500	17	2	1,500	750	1.50	11.76	18	0.1
Be-------	NM	15	17	1	15	15	1.00	5.88	5.9	0.1
Bi-------	M	50	18	1	50	50	1.00	5.56	5.6	0.1
							Total Magnitude (EM)----------		5,736	

Hanover-Fierro district

Cu-------	M	100	13	11	15,900	1,445	14.45	84.62	1223	24.6
Cu-------	NM	100	13	11	8,850	805	8.05	84.62	681	13.7
Mo-------	NM	50	13	5	3,700	740	14.80	38.46	569	11.4
Pb-------	NM	500	13	8	35,200	4,400	8.80	61.54	542	10.9
Bi-------	NM	50	13	3	2,250	750	15.00	23.08	346	7.0
Mn-------	M	2,000	13	13	72,000	5,538	2.77	100.00	277	5.6
Co-------	M	50	13	13	940	72	2.41	100.00	241	4.8
Ag-------	NM	5	13	4	145	36	7.25	30.77	223	4.5
Zn-------	M	500	13	7	10,900	1,557	3.11	53.85	168	3.4
Zn-------	NM	500	13	3	9,500	3,167	6.33	23.08	146	2.9
Sn-------	NM	100	13	4	1,650	412	4.13	30.77	121	2.6
Au-------	NM	20	13	1	200	210	10.00	7.69	77	1.5
Mg-------	NM	1.5	13	5	14	2.8	1.87	38.46	72	1.4
Mg-------	M	1.5	13	6	13	2.2	1.50	46.15	69	1.4
Co-------	NM	30	13	5	230	46	1.53	38.46	59	1.2
Ba-------	NM	2,000	13	2	12,000	6,000	3.00	15.38	46	0.9
Mn-------	NM	2,000	13	3	9,000	3,000	1.50	23.08	35	0.7
Pb-------	M	500	13	3	1,500	500	1.00	23.08	23	0.5
V--------	M	500	13	2	1,200	600	1.20	15.38	18	0.4
W--------	NM	100	13	2	200	100	1.00	15.38	15	0.3
W--------	M	100	13	1	150	150	1.50	7.69	12	0.2
Mo-------	M	50	13	1	50	50	1.00	7.69	7.7	0.2

Total Magnitude (EM)----------4,971

TABLE 3.—*Comparison of magnitudes for selected metals—Continued*

Element	Concentrate fraction	Threshold value	Number of samples	Number of anomalous samples	Sum of anomalous values	Mean anomalous value	Intensity (mean/ threshold)	Area (percent anomalous)	Magnitude (EM) (Intensity X Area)	REM (cumulative percent magnitude)
				Shingle Canyon district						
Pb-------	NM	500	17	11	86,000	7,818	15.64	64.71	1,012	25
Co-------	M	30	17	17	2,970	175	5.82	100.00	582	15
Zn-------	M	500	17	15	31,100	2,073	4.15	88.24	366	9.2
Cu-------	NM	100	17	12	6,150	512	5.13	70.59	362	9.1
Mn-------	M	2,000	17	13	80,000	6,154	3.08	76.47	235	5.9
Cu-------	M	100	17	13	3,650	281	2.81	76.47	215	5.4
V--------	NM	500	17	9	18,200	2,022	4.04	52.94	214	5.4
Mg-------	M	1.5	17	6	45	7.5	5.00	35.29	176	4.4
Zn-------	NM	500	17	9	14,000	1,556	3.11	52.94	165	4.1
Mo-------	NM	50	17	3	1,270	423	8.47	17.65	149	3.8
Ag-------	NM	5.0	17	4	90	22	4.50	23.53	105	2.7
Pb-------	M	500	17	7	8,700	1,243	2.49	41.18	102	2.6
Mn-------	NM	2,000	17	8	28,000	3,500	1.75	47.06	82	2.1
Co-------	NM	30	17	5	350	70	2.33	29.41	69	1.7
V--------	M	500	17	7	4,600	657	1.31	41.18	54	1.4
Mg-------	NM	1.5	17	1	5	5.0	3.33	5.88	20	0.5
Sn-------	NM	100	17	1	300	300	3.00	5.88	18	0.4
Ba-------	NM	2,000	17	1	5,000	5,000	2.50	5.88	15	0.4
Bi-------	NM	50	17	1	100	100	2.00	5.88	12	0.3
Be-------	NM	15	17	1	15	15	1.00	5.08	5.9	0.1
Bi-------	M	50	17	1	50	50	1.00	5.88	5.9	0.1
Mo-------	M	50	17	1	50	50	1.00	5.88	5.9	0.1
						Total Magnitude (EM)----------			3,971	

Juniper Hill district

Ag-------	NM	5	77	12	2,270	189	37.83	15.58	590	23
Pb-------	NM	500	77	14	147,500	10,536	21.07	18.18	383	15
Co-------	M	30	79	69	5,420	79	2.62	87.34	229	9.0
Mg-------	M	1.5	79	50	261	5.2	3.49	63.29	221	8.7
Mn-------	M	2,000	79	60	346,000	5,767	2.88	75.95	219	8.6
Mg-------	NM	1.5	77	23	190	8.3	5.51	29.87	164	6.5
V--------	M	500	79	58	45,900	791	1.58	73.42	116	4.6
Zn-------	M	500	79	46	42,800	930	1.86	58.23	108	4.3
Zn-------	NM	500	77	11	35,000	3,819	6.36	14.29	91	3.6
Mo-------	NM	50	75	7	3,240	463	9.26	9.33	86	3.4
Pb-------	M	500	79	17	33,200	1,953	3.91	21.52	84	3.3
Ba-------	NM	2,000	77	18	86,000	4,778	2.39	23.38	56	2.2
Ba-------	M	2,000	79	19	59,000	3 105	1.55	24.05	37	1.5
V--------	NM	500	77	11	11,900	1 082	2.16	14.29	31	1.2
Mo-------	M	50	79	8	740	92	1.85	10.13	19	0.7
Mn-------	NM	2,000	77	8	25,000	3,125	1.56	10.39	16	0.6
Cu-------	NM	100	77	7	1,250	179	1.79	9.09	16	0.6
Cu-------	M	100	79	9	1,250	139	1.39	11.39	16	0.6
Ag-------	M	5	79	7	53	7.6	1.51	8.86	13	0.5
Be-------	M	15	79	7	130	18.6	1.24	8.86	11	0.4
W--------	M	100	79	3	600	200	2.00	3.80	7.6	0.3
Au-------	NM	20	77	2	80	40	2.00	2.60	5.2	0.2
Bi-------	NM	50	77	2	200	100	2.00	2.60	5.2	0.2
W--------	NM	100	77	3	300	100	1.00	3.90	3.9	0.2
Be-------	NM	15	77	2	30	15	1.00	2.60	2.6	0.1
Co-------	NM	30	77	2	60	30	1.00	2.60	2.6	0.1
Sn-------	NM	100	77	1	100	100	1.00	1.30	1.3	0.1

Total Magnitude (EM)---------- 2,534

TABLE 3.—*Comparison of magnitudes for selected metals—Continued*

Element	Concentrate fraction	Threshold value	Number of samples	Number of anomalous samples	Sum of anomalous values	Mean anomalous value	Intensity (mean/ threshold)	Area (percent anomalous)	Magnitude (EM) (Intensity X Area)	REM (cumulative percent magnitude)
					Skate Canyon					
Co	M	30	25	25	4,870	195	6.49	100.00	649	29
Mg	M	1.5	25	25	146	5.8	3.89	100.00	381	18
Mn	M	2,000	25	16	129,000	8,063	4.03	64.00	258	12
V	M	500	25	24	23,000	958	1.92	96.00	184	8.4
Zn	M	500	25	19	17,900	942	1.88	76.00	143	6.5
Mg	NM	1.5	25	10	40	4.0	2.70	40.00	108	4.9
Ba	M	2,000	25	7	54,000	7,714	3.86	28.00	108	4.9
Sn	NM	100	25	3	1,900	633	6.33	12.00	76	3.5
Mn	NM	2,000	25	11	32,000	2,909	1.45	44.00	64	2.9
Co	NM	30	25	3	380	127	4.22	12.00	51	2.3
Cu	M	100	25	6	1,250	208	2.08	24.00	50	2.3
Cu	NM	100	25	4	1,150	287	2.88	16.00	46	2.1
Pb	NM	500	25	2	3,000	1,500	3.00	8.00	24	1.1
V	NM	500	25	4	2,700	675	1.35	16.00	22	1.0
Be	NM	15	25	4	70	17	1.17	16.00	19	0.8
Ba	NM	2,000	25	1	2,000	2,000	1.00	4.00	4.0	0.2
Zn	NM	500	25	1	500	500	1.00	4.00	4.0	0.2
						Total Magnitude (EM)----------			2,199	

Sheep Corral Canyon

Mg------	M	1.5	41	38	310	8.2	5.45	92.68	505	26
Co------	M	30	41	41	4,570	111	3.72	100.00	372	19
Mn------	M	2,000	41	36	242,000	6,722	3.36	87.80	295	15.3
Sn------	NM	100	41	7	5,600	800	8.00	17.07	137	7.1
Zn------	M	500	41	22	23,000	1,045	2.09	53.66	112	5.8
V-------	M	500	41	31	22,300	719	1.44	75.61	109	5.6
Mg------	NM	1.5	41	7	57	8.1	5.43	17.07	93	4.8
Bi------	NM	50	41	2	1,800	900	18.00	4.88	88	4.6
Cu------	M	100	41	16	2,750	172	1.72	39.02	67	3.5
Ba------	NM	2,000	41	12	36,000	3 000	1.50	29.27	44	2.3
Co------	NM	30	41	5	430	86	2.87	12.20	35	1.8
Cu------	NM	100	41	5	1,000	200	2.00	12.20	24	1.3
Pb------	NM	500	41	5	4,400	880	1.76	12.20	21	1.1
Mn------	NM	2,000	41	2	10,000	5,000	2.50	4.88	12	0.6
Ba------	M	2,000	41	1	5,000	5,000	2.50	2.44	6.1	0.3
Mo------	NM	50	41	1	70	70	1.40	2.44	3.4	0.2
V-------	NM	500	41	1	700	700	1.40	2.44	3.4	0.2
Be------	NM	15	41	1	15	15	1.00	2.44	2.4	0.1

Total Magnitude (EM)---------- 1,929

Element	Concentrate fraction	Threshold value	Number of samples	Number of anomalous samples	Sum of anomalous values	Mean anomalous value	Intensity (mean/ threshold)	Area (percent anomalous)	Magnitude (EM) (Intensity X Area)	REM (cumulative percent magnitude)
				Circle Mesa						
Co-------	M	30.0	21	21	1,610	77	2.56	100.00	256	19
Ba-------	M	2,000.	21	16	79,000	4,937	2.47	76.19	188	14
Mn-------	M	2,000.	21	10	68,000	6,800	3.40	47.62	162	12
W--------	M	100.	21	12	2,950	246	2.46	57.14	140	10
Sn-------	NM	100.	21	6	2,700	450	4.50	28.57	129	9.5
V--------	NM	500.	21	21	11,600	553	1.10	100.00	110	8.2
Ba-------	NM	2,000.	21	5	40,000	8,000	4.00	23.81	95	7.0
Zn-------	M	500.	21	17	9,400	552	1.11	80.95	90	6.6
Pb-------	M	500.	21	10	8,100	810	1.62	47.62	77	5.7
Cu-------	M	100.	21	7	800	114	1.14	33.33	38	2.8
Mn-------	NM	2,000.	21	3	8,000	2,667	1.33	14.29	19	1.4
Zn-------	NM	500.	21	3	1,700	567	1.13	14.29	16	1.2
Cu-------	NM	100.	21	1	150	150	1.50	4.76	7.1	0.5
Be-------	M	15.	21	1	20	20	1.33	4.76	6.4	0.5
Be-------	NM	15.	21	1	15	15	1.00	4.76	4.8	0.4
Mo-------	NM	50.	21	1	50	50.000	1.00	4.76	4.8	0.4
V--------	NM	500.	21	1	500	500.000	1.00	4.76	4.8	0.4
W--------	NM	100.	21	1	100	100.000	1.00	4.76	4.8	0.4
						Total Magnitude (EM)----------				1,348

TABLE 4.—*Additive ratios of element magnitudes (EM)*

[EM = Intensity × halo size (area). Leaders (---) indicate no value calculated]

Area	[1]Pb + Ag + Ba / Cu + Mo + Bi
Georgetown district	14.78
Fleming Camp area	12.82
Chloride Flat-Boston Hill district	10.26
Juniper Hill district	9.54
Circle Mesa	8.00
Shingle Canyon district	3.89
Central district	1.54
Pinos Altos district	1.50
Fierro-Hanover district	0.51
Skate Canyon[2]	---
Sheep Corral Canyon[2]	---

[1]Nonmagnetic component.

[2]Statistically nonsignificant due to insufficient number of values.

☆ U. S. GOVERNMENT PRINTING OFFICE: 1984—776-041/4021 REGION NO. 8